Active Temperature Control Algorithms for Improved Reliability and Lifetime of Photovoltaic Power Converters

RENATO JACOBO-TAPIA

Active Temperature Control Algorithms for Improved Reliability and Lifetime of Photovoltaic Power Converters

Renato Jacobo-Tapia

Submitted for the degree of Master in Science by Research

Abstract

Power converters are exposed to environmental stresses that affect reliability. Among these, ambient temperature and solar irradiance are the ones that affect photovoltaic (PV) systems the most. For solar irradiance this is especially true for days with dynamic irradiance like those with variable cloud conditions. The power conversion is not perfect and has power losses that heat up the components. Among the most fragile components in power converters are power semiconductors and capacitors, which are greatly affected by thermal variations. This thesis presents temperature control algorithms to enhance reliability and lifetime of PV converters. The algorithms are focused on thermal control through duty cycle regulation. The first one is called temperature-controlled (TC) maximum power point tracking (MPPT) algorithm and is used for lifetime improvement of PV converters under dynamic irradiance conditions during cloudy days. The second is called maximum-temperature-limited (MTL) MPPT algorithm and is used to improve the lifetime of PV converters by limiting the output power during days with high irradiance and high ambient temperature levels. The effectiveness of the algorithms is verified using extensive simulations, evaluating the lifetime and comparing it with the energy generated. For the TC MPPT, the evaluation is done under daily irradiance profiles for different cloud conditions, while for the MTL MPPT a maximum temperature is set to test during a yearly mission profile. The results show that the TC MPPT algorithm managed to reduce life consumption by 4.68% with 0.08% of energy reduction for very variable cloud condition days. Moreover, the MTL MPPT algorithm reduced the yearly life consumption by 28.36% with a small energy generation cost of 3.97%. Based on these results it is possible to validate the effectiveness of thermal management strategies, which apart from enhancing energy production with no extra hardware cost can improve reliability at the same time.

Active Temperature Control Algorithms for Improved Reliability and Lifetime of Photovoltaic Power Converters

Renato Jacobo-Tapia

A Thesis presented for the degree of
Master in Science by Research

Future Energy Systems
Department of Engineering
University of Durham
United Kingdom

September 2021

Contents

List of Tables

List of Figures

Declaration

The work in this thesis is based on research carried out at the Future Energy Systems, the Department of Engineering, United Kingdom. No part of this thesis has been submitted elsewhere for any other degree or qualification and it is all my own work unless referenced to the contrary in the text.

Acknowledgements

Thanks to God.

Afterwards, I would like to thank my wife Magdalena, without all her support, strength, kindness and love I would not have been able to achieve my master degree. Then I would like to thank my mother for her support, counseling and for always show interest in my well-being. My father that have always support me in all possible ways. My sisters Dirce and Kenia, where I can find support whenever I need it.

I would also like to thank the friends I made in this part of the journey, Eduardo G. and Hector for those walks and talks about everything. Julie and Megan for their happiness, for sharing their own cultures and learn about mine. Rodrigo and Eduardo B. for always improve the mood with some good food or pastries. Cesar for always be ready for a monopoly game. David B. for all the support and counseling with the paper work apart of being fun and positive. Lydia for those game-nights, the culture, the food and all those exciting trips in the nature, ruins and castles. Xinyi Zhu for sharing her culture, those gifts exchanges and the love for Harry Potter. My desk-mate Nadia for being a friendly person and give lots of tips and good suggestions. My housemates, Cerise for being a really good English teacher, for being a fun and positive person and for that nice bicycle. Julia for being a kind person, for helping me to improve my English and for the Netflix user. Flora and David for those game-nights, food and some good laughs.

Thanks to friends from before, who have influence me to be who I am. From university, Giovanny, Jose M., Rulber and Denisse. From high school Eduardo, Vladimir, Ulises, Omar, Jorge, Uriel and Evelyn. From middle school Sergio and especially Alicia who has always been near and even when I get distant she has kept our friendship alive.

Finally I would like to thank all the professors that have marked my life for good. To my supervisor Mahmoud Shahbazi for the support, counseling and all the time he has invested to help me complete my degree, among other things that have been important in this path. To Victor Hugo Sosa for applying some pressure on me, for teaching me how to search and how to write. To Antonio Medina for being always a kind and selfless person. To Miguel Angel Lopez for teaching me discipline, fitness and optimism.

Thanks to all of them.

This poem has gave me lots to think about. Every time I feel I am over-focusing in the outcome and no the path I come back to read it again.

"Always in your mind keep Ithaca.
To arrive there is your destiny.
But do not hurry your trip in any way.
Better that it last for many years;
that you drop your anchor at the island an old man,
rich with all you've gotten on the way,
not expecting Ithaca to make you rich.

Ithaca gave you the beautiful journey;
without her you wouldn't have set upon the road.
But now she has nothing left to give you.

And if you find her poor, Ithaca didn't deceive you.
As wise as you will have become, with so much experience,
you will understand, by then,these Ithacas; what they mean." - Cavafy.

Dedicated to

My beloved wife, family and friends

Chapter 1

Introduction

Nowadays, renewable energy systems are of great use to combat climate change and to limit global warming. To limit the effects of global warming the reduction of greenhouse gas (GHG) emissions generated by humans is of critical importance. In this concern, renewable sources of energy such as wind and solar are in a good position as they can be used to help to shift from carbon-based to cleaner energy sources. Nevertheless, it is important to remark that more research is needed to reduce the cost of renewable sources and make them more competitive [1]. Among the different renewable energy systems, Photovoltaic (PV) energy has seen a sharp growth in recent years [2] and is especially important due to its great availability in many parts of the world. One major drawback for PV energy is the high installation cost compared with carbon-based energy sources. Therefore, it is important to reduce costs on this type of energy systems. PV energy is composed of solar panels and power converters. Solar panel technology is developing fast, with prices dropping and reliability levels improving at good rates [3]. The reliability problem for PV energy system comes with PV converters, which are costly, are subject to several environmental stressors and have low-reliability levels accounting for 37% of failures and 59% of unscheduled maintenance costs among the components of a PV systems [4], see Fig. 1.1 for reference.

Solar panels function in PV systems are to transform energy from the sun into electricity. Solar panels do not have movable parts and have few components, which make them have good reliability levels. The function of power converters in PV

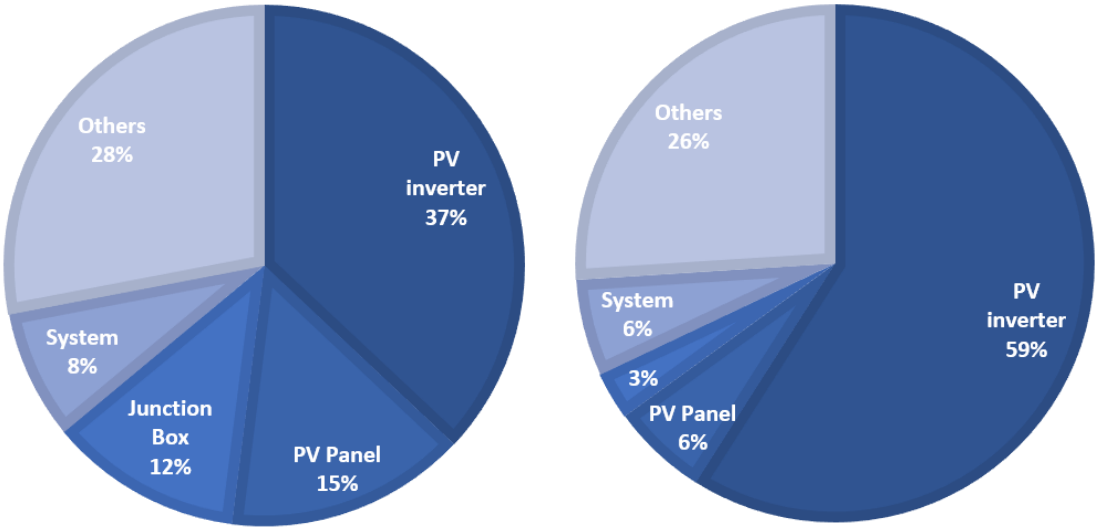

(a) Failure events

(b) Maintenance costs

Figure 1.1: Percentage of failure events (a) and maintenance costs (b) for PV inverters *Figures created based on information from [4]

systems is to transform the DC electricity generated by the solar panels into usable and controlled AC electricity and feed a load or inject it to the grid. Although PV converters do not have movable parts, they are composed of many elements and are subject to more stresses than solar panels due to power management and electric losses, which affects the overall system reliability [5]. One of the main causes that affect the reliability of power converters in PV systems is thermal cycling [6]. Ambient temperature and solar irradiance variations are among the principal agents causing thermal cycling in these systems and will be addressed by this work. Among the components with the lower reliability levels in PV converters are capacitors and power semiconductors [7]. Power semiconductors were highlighted by industry experts as the most crucial elements of the system and it was suggested to focus more research in this area [8] [9]. This work therefore will focus on the impact that power semiconductors have in the lifetime of power converters, particularly IGBT switching devices.

During their operation, PV power converters are exposed to stressors such as ambient temperature, solar irradiance, humidity, vibrations and dust, among others. Ambient temperature and solar irradiance are of special interest, as they have a direct impact on the thermal cycling which affects the reliability of power electron-

ics [10]. Another issue that affect the reliability of PV converters is the constant variations of irradiance during days with passing clouds [11]. In a day with clear sky, the solar irradiance affects the reliability of the system in the form of available power due to power losses in the IGBT devices. For days with dynamic cloud conditions, the constant change in solar irradiance and available power leads to further thermal cycling. The reliability and lifetime of power electronics can be evaluated through the analysis of thermal cycling, which have been broadly studied and strategies to evaluate it are available. Power generation of PV systems is also obviously directly dependant on solar irradiance levels. Furthermore, power electronics experience power losses during their operation, which heat up the devices causing thermal cycling, therefore, with higher irradiance levels, a higher temperature may be reached by switching devices. Moreover, the ambient temperature is involved in the temperature reached by the switching devices as the heat dissipation is directly affected by the ambient temperature.

The thermal cycling of power electronic IGBT devices leads to bond wire fatigue, which is a cause of failure [12]. The damage experienced by IGBT devices with temperature cycling is not linear [13]; the damage caused by higher thermal stresses is exponentially higher than that caused by lower thermal stresses. Moreover, as the power generation of power converters leads to thermal cycling, a reduction in the output power means a reduction in the thermal cycling of the IGBT devices [14]. As this relationship is almost linear, a small reduction in energy production is translated into great reductions in the life consumption of the switching devices. Therefore, one way to improve the lifetime of PV converters is to apply thermal management strategies in their control.

Based on the evidence that thermal stresses affects the lifetime of power electronics, this work suggests and addresses the following question: What are the advantages of using thermal management strategies for the lifetime improvement of PV systems? To answer this question, the state of the art regarding this topic will be presented and discussed in the following chapter, as well as an analysis of the characteristics and the applicability of these strategies on PV power converters. Furthermore, the next research question that this work tries to study is: How to

actively manage the temperature variation in power electronics, while keeping the output power almost constant? To address this question, this work proposes and tests two thermal management strategies to improve the lifetime of IGBT devices for PV systems. The thermal management methods will be applied in the control system of a two-stage PV power converter, with no extra hardware cost. This thermal control strategies leads to another question: What is the lifetime reduction impact that a thermal control strategy will have on a PV inverter for field operations? To answer this, the lifetime impact evaluation of the proposed control methods will be carried out with the help of extensive simulations in Matlab and Simulink environments. The first control method is intended to reduce the damage received by IGBT devices during dynamic irradiance conditions on cloudy days. The second method will reduce the maximum temperature reached by IGBT devices to reduce the impact received during days with high irradiance and high ambient temperature levels.

To analyze the effectiveness of the proposed control methods it is necessary to evaluate the reliability of the PV system. In this work, the reliability analysis will be focused on IGBT devices and the analysis of other power electronics components and capacitors are out of the scope of this work. For the study of the reliability of IGBT devices, an empirical lifetime model will be applied. The lifetime model applied in this work will be the Bayerer´s model which will be justified and explained in Chapter 2 and 3 respectively. Such model will evaluate the lifetime consumption of the IGBT devices for the given mission profiles (Solar irradiance and ambient temperature). The lifetime model will be applied to evaluate the damage received by a PV system with the proposed control strategies and compared with the damage received with a normal control strategy to find to what extent the proposed control strategies improve the reliability of IGBT devices in a PV system.

The rest of this work is organized as follows: the literature review is detailed in Chapter 2. In Chapter 3, the steps necessary to apply a lifetime modelling technique will be explained. The lifetime modelling will include the electrical design of a PV system in Matlab Simulink, the power loss estimation of the IGBT switching devices; the use of a thermal equivalent model to calculate the junction temperature of

the IGBT devices, a rainflow counting algorithm to organize the temperature cycles, the empirical lifetime model to calculate the remaining useful lifetime and a Monte Carlo simulation for the reliability calculation of the PV system. In Chapter 4, two modified maximum power point tracking (MMPT) algorithms are proposed, the first one controls the temperature change rate of IGBT devices under different cloud conditions, the second one limits the maximum junction temperature of IGBT devices, which can be used for device protection and damage reduction for days with high irradiance and high ambient temperatures. In Chapter 5, a PV system is designed and used to test the performance with the application of the modified algorithms, the empirical lifetime model is applied to evaluate the lifetime consumption of the PV system under normal operating conditions and compared with the application of the modified algorithms. Finally, the conclusions of this work are given in Chapter 6.

Chapter 2

Literature Review

In this Chapter the relevant information about reliability and lifetime evaluation of power electronics will be presented, especially the information related to solar applications. First, the concept of reliability in power electronics will be explained, as well as the current problems that the industry face for different applications and how to overcome them. Then, the reliability analysis of photovoltaic systems will be further analysed, considering what are the specific challenges the need to be solved. Afterwards, different studies that use the lifetime and reliability analysis for PV systems are reviewed, presenting the gaps that this work is discussing. Next, a problem faced by PV system is discussed, the negative effect that thermal cycling have in the reliability of PV converters. Dynamic irradiance conditions during cloudy days can be a cause for thermal cycling as well as days with high irradiance and high temperature levels. The study and analysis of these problems can be used to improved the reliability and lifetime levels of power electronics. Finally, the available strategies to evaluate reliability and lifetime of power electronics are presented and compared, with the aim to use the method most suitable for the specific challenges faced by power electronics in PV applications.

2.1 Reliability of power electronics

Reliability is defined as the probability that an item will perform a specific function without failure for a certain period of time [15]. Low reliability levels come with early

failure of components and increased system costs, therefore increasing reliability levels is an important task for manufacturers to reduce warranty costs and improve customer satisfaction [16].

Power electronics role in the generation and management of energy has increased drastically in recent years [7]. With the application of power electronics, the efficiency of electric systems has improved and a more flexible control is allowed in these systems [17]. However, due to the complexity of power electronic systems, reliability issues arise, which affects their implementation costs and life expectancy [18]. To meet industry and customer demands, more severe reliability requirements are being applied to power electronics systems [15].

Power electronics have multiple applications, such as aircraft, automotive, motor drives, railway, wind turbines, photovoltaic (PV) among others [15]. Power electronics reliability is affected by the specific working environments of each application. These working environments are the source of different kind of stressors, such as humidity, high temperature, vibrations, temperature cycling and dust, among others [19] which threaten reliability and can cause early failures. For renewable energy applications (e.g.photovoltaic and wind energy) this is especially true, as the performance of these systems is directly affected by meteorological conditions such as wind speed, ambient temperature or solar irradiance.

To overcome these issues the industry is changing to a Design for Reliability (DfR) process [18] where the reliability analysis of power electronics systems is executed during the design phase instead of testing for reliability afterwards, improving reliability levels without compromising cost and security. The application of the DfR process includes a broad analysis of the reliability of power electronics at the device level and system level. Moreover, it can be applied to study the effect that control strategy, topology selection or mission profile will have in the lifetime and reliability of power electronics [20].

2.2 Power electronics reliability in photovoltaics systems

Photovoltaic (PV) energy system has seen vast growth in recent years [2], which can be related to certain factors like the cost reduction, increased efficiency and the need to shift to clean energy sources to fight climate change [7]. Although PV energy seems promising, it may face problems that affect its reliability in some operation environments [8]. For the case of PV energy, the reliability can be affected principally by solar irradiance and ambient temperature changes. Therefore, the application of DfR in PV system can be beneficial to achieve lower costs and enhance reliability.

With the increasing participation of PV energy in modern energy systems, the reliability and lifetime of PV systems have become more important than ever. PV systems are comprised of two main components, solar panels and PV inverters (Fig. 2.1). PV systems are designed with lifetime targets of 30 years [15], which are being principally limited by the comparatively low reliability levels of power converters. While solar panels have high reliability levels and long warranties of 25 years [21], the power converters can reach a maximum of 15 years warranties due to the lower reliability levels [22]. Furthermore, in PV systems, the inverter accounts for 37% of failures [4] and the reliability improvement at component level (e.g. semiconductors, capacitors, gate-drives, cooling system and control unit) is crucial [7]. In power electronics systems, such as PV inverters, 31% of failures are caused by problems related to power semiconductors, 18% by capacitors and 15% by gate drive failures [9]. In surveys from industry experts, power semiconductors were pointed out as the most critical components and need to be appointed for reliability improvement [8] [9]. What is more, the inverter failures in PV systems account for 58% of maintenance costs [15], therefore improving reliability levels and reducing failure rates would reduce maintenance cost as PV inverters are costly. For these reasons, PV converters are the root of reliability issues in PV systems, thus, there are good opportunities to reduce costs and improve the reliability of these elements.

PV converters reliability is greatly affected by some of the environmental stressors mentioned above, principally by the ambient temperature and solar irradiance

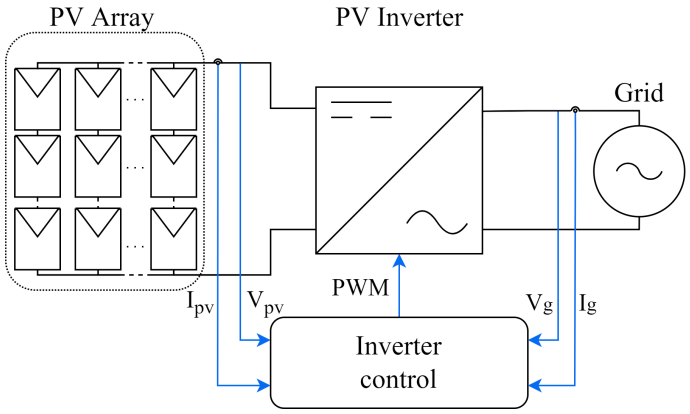

Figure 2.1: Basic diagram of a PV System, main elements: PV array and PV Inverter

changes. The change in ambient temperature has a direct impact on the temperature cycling experienced by PV inverters as it changes the temperature surrounding the devices which affect the heat dissipation. With changes in solar irradiance the available power changes too and these available power variations leads to variations in thermal losses during the system operation. As thermal cycling is one of the main reasons for failure in power switches [23], the study of thermal cycling caused by variations in ambient temperature and solar irradiance is crucial to improve the reliability of PV inverters. For example, one of the principal failures mechanisms in insulated-gate bipolar transistors (IGBTs) devices, widely used in PV inverters, is bond-wire fatigue caused by cycling variations in temperature, such as junction temperature (T_j) and temperature differential (ΔT_j) [24], which makes them the most fragile parts of modern PV systems.

Based on the aforementioned problems, it is clear that improving the reliability and lifetime of power converters, while not incurring higher costs is important. This can be achieved with different strategies as with the evaluation of control strategies, thermal management and topology selection [7]. As thermal stress is one of the principal causes of failure in power electronic components [25], thermal management strategies are a valuable option to achieve it. This work will analyse thermal management control strategies for lifetime and reliability improvement of PV systems. In Chapter 4 two control strategies focused in temperature management will be presented and a lifetime evaluation of these strategies will be implemented in Chapter 5. In the next section various works applying a lifetime estimation will be

presented and discussed.

2.3 Lifetime evaluation of photovoltaic systems

In the literature, lifetime evaluation of power electronics has been applied for different specific problems related to PV energy applications. Some of the most important findings are listed below:

- The analysis of the impact that the degradation of PV solar modules will have in the lifetime and reliability of a power converter is done in [22]. It was found that the life consumption of a PV system is reduced with the degradation of PV modules trough time, thus, not considering solar panel degradation leads to pessimistic lifetime calculations and can affect costs with over-designed items.

- The investigation of the effect of PV array sizing on the energy generated and the lifetime improvement of a PV system is presented in [14]. In this research PV arrays are over and under-designed to evaluate the impact that it will have on the reliability of PV inverters. It was found that the trade-off between lifetime and energy generated can be positive with the over-sizing of PV inverters in locations with low yearly solar irradiance levels. This is because the PV system works at underrate levels during most of the time of the year, so they will be capable to produce more energy with a small lifetime reduction.

- The study of PV panel positioning impact on lifetime is carried out in [26]. It was found that tilt angle of the PV modules have little effect in lifetime, while the orientation has a considerable impact and can be considered to improve the lifetime.

- The assessment of lifetime estimation has been also applied to a PV system with power limitation for lifetime target achievements in [27]. In this work PV systems on different mission profiles are tested and the lifetimes are evaluated. If the calculated lifetime is under the expected target, the production is reduced to increase the lifetime of the PV power converter, this way the

converter can cover the entire lifespan of the system at the cost of overall energy yield reduction. Inversely if the lifetime is over the target, the energy production is increased so the energy yield during the expected lifespan of the system is increased.

- The evaluation of lifetime modelling can be seen in micro-grid systems in [28]. In this study the effect of mission profile in the lifetime of the different subsystems are analysed, including a PV subsystem.

- The application of an optimized MPPT algorithm for lifetime improvement is discussed in [29]. Such algorithm controls the temperature change rate on PV systems, resulting in lifetime improvement and a slight power reduction.

There are various MPPT algorithms for harvesting the maximum energy possible in PV systems [30]. However, most of them have not taken into account the impact that dynamic irradiance conditions (e.g. fast changing cloud conditions) has on the lifetime impact of PV converters. Although the algorithm presented in [29] takes this into account, still it can be improved by making it faster and more efficient without compromising effectiveness. Such improvements are part of various important factors for MPPT algorithms, such as speed, complexity, cost and reliability [31]. The algorithm presented in this work addresses directly the speed and complexity of the algorithm and cost reductions and reliability improvements as byproducts of its application. Moreover, although the algorithm in [29] has been tested under a designed mission profile, it is important to point out the lack of a field operation mission profile verification. This should be considered relevant as the algorithm is intended for real life applications where the power converters have low reliability levels and high costs [4]. The proper analysis of the algorithm under a field operation mission profile is vital to understand its effects improving the lifetime and reducing costs.

These issues will be addressed by the first thermal management algorithm proposed in this study. This algorithm will be used to improve the lifetime and reliability of PV converters. It is important to note that thermal cycles have a huge impact on the lifetime of power converters [32], and they are greatly influenced by

solar irradiance and ambient temperature, which are the main components of a PV mission profile [22]. This means that the reliability and lifetime assessment under the field operation profile is crucial for a correct estimation of the impact that a temperature controlled MPPT algorithm can achieve. Moreover, the works in [27] and [14] rely on a power limitation to regulate the lifetime impact on PV system. To achieve this, the MPP tracking is shifted by regulating the required input voltage of the converter based on the maximum power allowed. The main drawback of this strategy is that it does not consider the ambient temperature which is crucial for the temperature of the switching devices. To address this problem, the second thermal management studied in this work will implement a power control strategy that consider the influence of ambient temperature as well.

2.4 Cloud condition lifetime impact

As stated before, thermal stress is one of the main factors that affect the reliability of power electronics, especially in PV applications that are subject to ambient temperature and solar irradiance variations in working conditions. The power generation of PV systems depends directly on the solar irradiance received, therefore the thermal stress of the system is affected by solar irradiance changes.

The solar irradiance received by the system is influenced by the cloud conditions, while a clear day does not affect the solar irradiance received, a day with fast-changing cloud conditions continuously change the solar irradiance received by the system. The constant variation of the solar irradiance leads to heat up and cool down processes that raise further thermal stresses and affects the reliability of the system.

The fluctuation of irradiance conditions caused by changing irradiance conditions has a direct impact on the thermal stresses experienced by a PV system. The constant changes in irradiance cause greater thermal cycling stress like larger temperature differentials and shorter heating times. The thermal cycle heating time has a direct impact on the lifetime consumption of power electronics, the shorter the cycle heating time (T_{on}), the larger the lifetime consumption. Similar to this is

the impact that the temperature differential (ΔT_j) has in the lifetime, where higher values in the temperature differential have a greater impact on the lifetime consumption of power electronics. The impact that thermal stresses have on the lifetime of power electronics will be further explained in the next section.

2.5 Strategies to estimate lifetime

It is possible to evaluate the lifetime of power electronic through different methods, each of these methods have certain characteristics which makes them more suitable for specific applications. In this section these methods will be explained and compared to see which is the most suitable for lifetime evaluation of power electronics for solar applications. For the case of lifetime evaluation of solar system under different cloud conditions it is crucial to consider the damage caused by thermal parameters. The different methods to estimate the lifetime of power electronics can be categorized into three main types [24] which are: constant failure rate models, empirical lifetime models and physics-of-failure (PoF).

The constant failure rate models are a simple way to estimate the lifetime of power electronics. The military handbook (MIL-HDBK-217) and the IEC 61709 are examples of constant failure rate models [33]. They were created by a necessity to establish a method to estimate the reliability of electronic components [34]. The constant failure rate models, also known as handbook failure rate models, consider a constant failure rate (λ) for different electronic components. There are different types of stress factors (π) considered in these models like environmental factor (π_E), electrical stress (π_V), temperature stress (π_T) among others. The constant failure rate models are widely accepted due to their easy application. Although their acceptance and easy applicability, some of the handbook models have pessimistic reliability estimations and fail to consider the damage produced by temperature variations, which limits its applications to fields like wind or PV energy.

Empirical lifetime models are based on the statistical analysis of failure rate in power electronics such as IGBTs. For this type of model, several devices are tested under various application conditions, like different power and temperature cycling

parameters [35]. The devices are tested until failure and from the data obtained it is possible to estimate the impact that parameters such as junction temperature, temperature differential among others will have in the lifetime of IGBT devices [13]. The advantage of empirical lifetime models is that they consider the temperature cycling that the mission profile will cause in the system. One disadvantage is that empirical lifetime models give a statistical result, which is a good approximation but can not define exactly which would be the cause of failure. This type of model does not require a wide knowledge of the electronic materials and construction architecture to evaluate the lifetime and can be easily implemented with the help of parameters obtained from data sheets which make them very practical [36].

Another type of lifetime model is Physics-of-Failure (PoF). This kind of model considers the material characteristics and device structure to precisely define the cause of failure under specific stress characteristics [37]. They have the advantage of high precision, however, a deep knowledge of the device characteristics and materials is required, which makes their application more complex and relegates them to research purposes.

Among the different strategies to evaluate the lifetime of power electronics have been presented, each method has certain advantages and it can be said that none is the "best" overall. Therefore, it is necessary to consider the specific challenges of an specific application.

For the case of power electronics in PV systems, the constant failure rate methods are not suitable, as the analysis of thermal cycling in these systems is crucial. PoF models are viable option, but the detailed data and information necessary (material and construction knowledge for specific devices) makes it not the best option for this work. Empirical lifetime models are easy to implement, they also consider the impact caused by thermal cycling [24] and can be implement with the information obtained from data sheets as it is based in statistical information and not in a deep knowledge of specific devices. For the aforementioned causes, empirical lifetime models are the best option for this work. The Coffin–Manson model is one of the most used empirical lifetime models, it considers the temperature differential (ΔT_j). However, the Bayerer´s model also considers the cycle heating time (T_{on})

and junction temperature (T_j) [24], which makes it best suited for this study. The Bayerer´s model will be further explained in Chapter 3.5 and implemented in this work for the lifetime analysis of the PV system.

2.6 Summary

In this chapter the relevant information regarding reliability and lifetime analysis of power electronics has been discussed, with a focus on solar energy systems. Moreover, the main problems faced by power electronics and the strategies that are being taken to improve the reliability have also been shown. Different works have been displayed and discussed, which have used reliability analysis as a tool to help improving the lifetime of PV systems. Then, considering that temperature variations greatly affect the lifetime of power electronics in PV systems, a concerning issue about thermal cycling caused by dynamic cloud conditions have been pointed out. Further discussion about the cloud conditions topic and a technique to reduce the damage received by power electronics will be presented in Chapter 4. Finally, some methods to evaluated the lifetime were presented in this chapter, where an empirical lifetime model was selected and will be discussed in the next chapter.

Chapter 3

Lifetime modelling for power semiconductor switches in PV applications

In this chapter an empirical lifetime model will be explained. This lifetime model is an evaluation tool which will be used in the rest of this work. It is use to evaluate the damage received by power semiconductors in PV systems, it principally considers the damage impact of temperature variations. The evaluation can be applied to compare PV systems with different characteristics like size, devices used, positioning or PV systems with different control methods which is the case for this work. In Chapter 5, the model will be used to compare normal and modified MPPT control algorithms under irradiance profiles with different cloud conditions.

The empirical lifetime model aims to evaluate the damage received by the switching devices under specific mission profiles. To correctly assess the mission profile experienced by IGBT switching devices in a PV system, it is necessary to accurately model the system. To achieve this, Matlab along with Simulink are the tools used in this work to represent the PV system. With the use of such tools, it is possible to accurately simulate the behaviour and then evaluate the operation of the system.

In this chapter, the steps necessary to apply a lifetime model are described. First, the electrical model that simulates the behaviour of a PV system under solar irradiance profiles is presented. For this step an irradiance mission profile is fed

into the electrical model of a PV system in Matlab Simulink and relevant information of the system are obtained, such as the energy generated by the system and energy losses of the IGBT switches. Then the energy losses are used to estimate the temperature experienced by the IGBT devices during the mission profile with a thermal equivalent model [10]. Next, the temperature profile is processed by a rainflow counting algorithm that classifies the random thermal cycles [38]. Finally, with the organized thermal cycles the lifetime model is applied to estimate the lifetime consumption of the switching devices with the use of the Bayerer's model during the mission profile [13].

3.1 Electrical model

For this work, a grid-connected PV system has been designed in Matlab Simulink environment to simulate its behaviour under different solar irradiance profiles and obtain the necessary data, such as power generation and power losses. The designed system is composed of a PV array and a two-stage power converter connected to the grid (See Fig. 3.1).

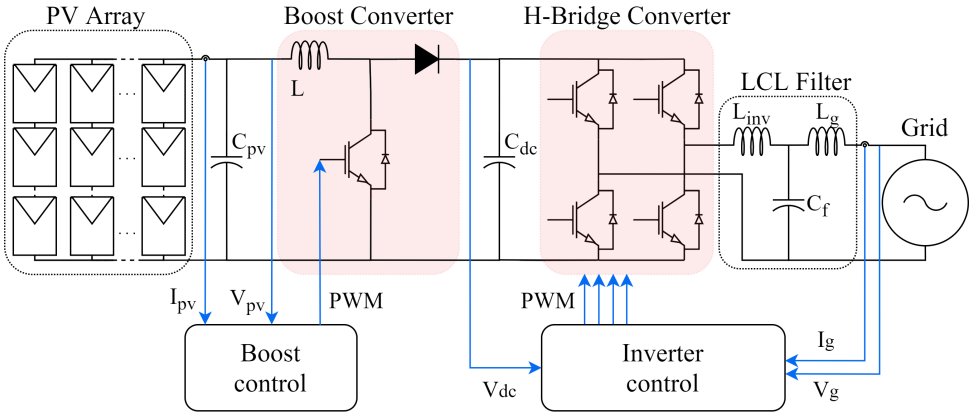

Figure 3.1: Electric diagram of the proposed PV system

The PV array is composed of a group of series and parallel connected solar panels. The two-stage power converter includes a boost converter in the first stage which is using a perturb and observe (P&O) maximum power point tracking (MMPT) control to maintain the voltage at the correct level in order to extract the maximum energy possible. The second stage is an H-bridge inverter that converts the direct

current (DC) from the solar panels into alternate current (AC) output. Moreover, the H-bridge converter is controlled by a phase-locked loop (PLL) which is used to synchronize the current injection with the grid frequency and allows the connection of the system to the grid.

3.2 Power losses

The operation of the electric system described above leads to energy dissipation. Both stages of the converter described above have an effect on the IGBT devices power losses, the first stage principally in the way of available power and the second stage in the way of sinusoidal current injection. Energy dissipation in power electronics is related to the harvested energy and the sinusoidal current injection which causes power cycling and lifetime reduction [39]. The analysis of the energy dissipated in electronic devices is especially important due to the lower reliability of IGBT devices compared with other elements in the system [4]. The power losses of IGBTs cause a rise in temperature that can lead to instant failure if a certain limit is exceeded or can lead to an early failure caused by the thermal stress experienced by the devices. To correctly estimate the lifetime it is necessary to estimate the power losses of IGBT devices during the operation of the system.

The power losses of the IGBT (3.1) are caused by conduction losses (3.2) and switching losses (3.3) [17]. The conduction losses are the result of the on-state operation of the IGBTs and are dependent on parameters such as on-state voltage (V_{ce}) and collector current (I_c). The switching losses take place during the transition of off-state to on-state and vice versa, and can be the principal source of losses. it is dependant on the switching frequency (f_{sw}), turn-on energy (E_{on}) and turn-off energy (E_{off}).

$$P_{IGBT} = P_{cond(IGBT)} + P_{sw(IGBT)} \tag{3.1}$$

$$P_{cond(IGBT)} = V_{ce} \cdot I_c \tag{3.2}$$

$$P_{sw} = (E_{on} + E_{off}) \cdot f_{sw} \tag{3.3}$$

Similarly to the IGBT losses, the diode losses require to be calculated as it has a direct impact on the temperature of IGBTs [39]. The total power losses of diode (3.4) is composed by conduction losses (3.5) and switching losses (3.6). The conduction losses are calculated based on the on-state voltage in the diode (V_d) and the current flowing through it (I). The switching losses are composed of the reverse recovery energy of the diode [17].

$$P_{Diode} = P_{cond(Diode)} + P_{sw(Diode)} \tag{3.4}$$

$$P_{cond(Diode)} = V_d \cdot I \tag{3.5}$$

$$P_{sw(Diode)} = (E_{rec}) \cdot f_{sw} \tag{3.6}$$

The basic principle for switching losses calculation explained above is applied in this work for simplicity, it considers constant switching losses. This might have an impact on the total losses of the system, although, as the system in this work is designed with a relatively low switching frequency this impact is not substantial (See Chapter 5 for more detailed system design information). However, in case of a more detailed and precise calculation needed, the formula should be normalized based on the specific device parameters and other variables such as DC-link and load current should be considered [39].

3.3 Thermal equivalent model

In practical applications the Solar inverter technology is shifting to the use of integrated modules instead of discrete devices [40]. Some integrated modules have temperature sensors embodied [41], these sensors are already in use (e.g. to limit the output power in case of overheating) and could be use for the application of the modified algorithm with no extra cost. This work will focus on simulation of discrete

devices to simplify the power losses and thermal modelling explanation, although the approach can also be applied to integrated modules. Once the power losses of the devices are calculated we use them to estimate the temperature changes of the IGBT devices. To achieve the temperature estimation an equivalent thermal model is applied in this work. Thermal equivalent models are used to calculate the thermal behaviour of materials with the help of an equivalent electric model [42] [43]. Thermal parameters are analogous to electrical parameters as seen in Table 3.1, thus the calculation of the junction temperature (T_j) of the switching devices is carried out with the application of an RC (resistor-capacitor) circuit.

Table 3.1: Electro-thermal analogy of thermal equivalent models

Electrical quantity	Units	Thermal quantity	Units
Potential difference	Volts (V)	Temperature difference	Kelvin (K)
Electrical resistance	Ohms (Ω)	Thermal resistance	(K/W)
Electrical current	Amps (I)	Power (Heat flow)	Watts (W)
Electrical capacitance	Farads (F)	Thermal capacitance	(J/K)

There are two basic configurations of thermal equivalent circuits which are Foster model Fig. 3.2a and Cauer model Fig. 3.2b [44]. The two models are precise but the complexity and applicability differ. The selection between one or another depends on the necessary results and data available [42].

Both models are composed of a current source representing the power dissipated (heat flow) by the power electronic devices, a group of series and parallel-connected resistors (R) and capacitors (C) that represent the material layers of the device and direct current (DC) source that represents the ambient temperature. The voltage measured between the current source and the ground point represents the T_j.

The Cauer model, also known as continued-fraction circuit gives a precise temperature estimation of the individual layers of the IGBTs, the main drawback of this model is that it requires a wide knowledge of the material characteristics and limits its application. An advantage of this model is the possibility to precisely estimate the temperature in specific points of the model which represent the individual layer materials of the device. The other type of thermal model, the Foster model, also known as partial-fraction circuit also gives a good estimation of the temperature.

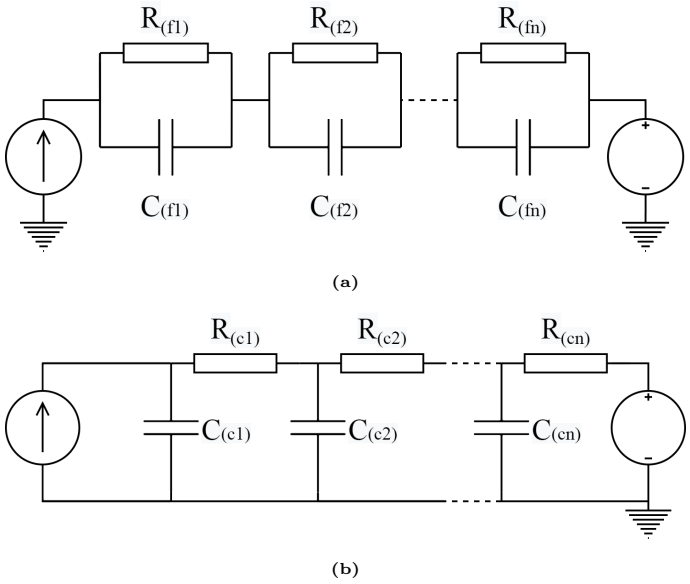

Figure 3.2: Foster(a) and Cauer(b) thermal equivalent models

The advantage of the Foster model is that it does not require deep knowledge of the layer materials to estimate the junction temperature. The require data can be extracted from the measured cooling curve of the device and is widely available in datasheets. Its principal drawback is that the model does not longer represent individual material layers and can only estimate the junction temperature T_j.

After the presentation and comparison of the thermal models. Considering the precision of the models, that for this work there is no need of temperature calculation of specific layers in the device and thanks to the easy access of data directly from datasheets, a Foster model is selected and will be used in this work for temperature calculation. Next, a rainflow counting algorithm is used to organized the temperature profile, the algorithm will be explained in the next section.

3.4 Rainflow counting

Lifetime modelling will handle the thermal cycles that occurred during the operation of the PV system, yet it is still necessary to organize the random thermal cycles of the temperature profile obtained from the thermal model. For this purpose, a rainflow counting algorithm is applied. A rainflow counting algorithm is a tool used to count and classify the stress-strain cycles in fatigue analysis [38]. In the case of power

electronics the rainflow counting algorithm is used to classify the temperature cycles by junction temperature (T_j), temperature differential (ΔT_j) and cycle heating time (T_{on}).

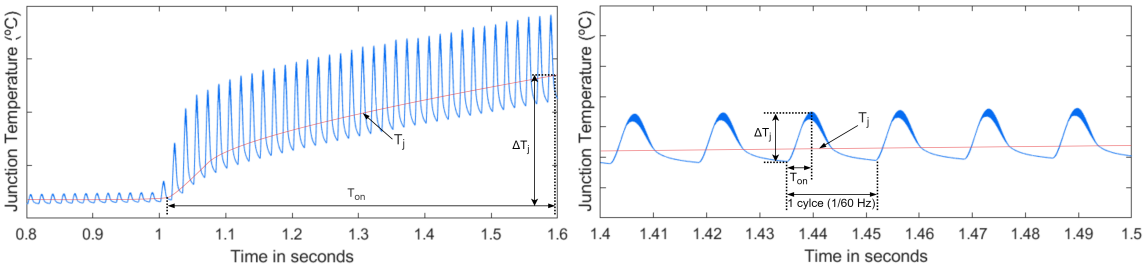

Figure 3.3: Representation of the temperature cycling experienced by an IGBT device during a change in irradiance conditions. Short-term temperature cycle can be seen in the zoomed area. T_j-Mean junction temperature, ΔT_j-Temperature differential, T_{on}- Heating time of the power cycling

In the temperature profile there are short-term and long-term temperature cycles. Short-term temperature cycles are in the order of millisecond and are caused mainly by the sinusoidal current injection to the grid, therefore the T_{on} matches with the fundamental frequency of the grid ($60Hz$). Long-term temperature cycle is in the range of second to the year time period and is influenced by the irradiance and ambient temperature [15]. An example of the temperature cycling experienced by an IGBT device can be seen in Fig. 3.3, where short and long term temperature cycles can be found.

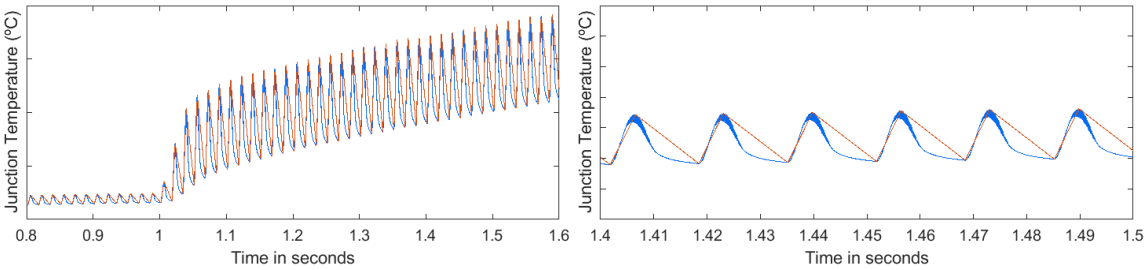

Figure 3.4: Representation of the application of the rainflow counting algorithm to find the peaks and valleys of the temperature cycling experience by an IGBT device during a change in irradiance conditions.

The rainflow counting in this work is applied with help of the "rainflow" function in Matlab. The temperature profile of the system can not be directly processed by the rainflow function. This is because the matlab function is not able to find the

peaks and valleys, it is just able to organise them. Therefore, it is necessary to find the peaks and valleys of the temperature profile. To do so, the profile is prepared with the aid of "findpeaks" Matlab function as seen in Fig. 3.4. The function processes the temperature profile and extracts the local maxima (peaks). To find the local minima (valleys), the temperature profile needs to be vertically flipped and the "findpeaks" function can be applied then. Peaks and valleys are then organized to apply the "rainflow" function (An example of the application of this function can be found in Chapter 5.1.2)

3.5 Lifetime modelling

An empirical lifetime model is applied in this work to evaluate the impact that different cloud conditions irradiance profile have in a PV system. Empirical lifetime models find good applicability in PV applications as these models consider the effect that thermal cycling has in the lifetime of power electronics, and not just the application and constant factors as the constant failure rate models [24]. For PV systems the consideration of thermal cycling in the lifetime estimation is crucial. This is because mission profile factors such as ambient temperature and solar irradiance change constantly, which have an impact on thermal cycling and therefore in the reliability.

The lifetime model applied in this work is the Bayerer's lifetime model [13] which is based on statistical analysis of power electronics, where 3.7 is the corresponding equation. It considers thermal variables such as junction temperature (T_j), temperature differential (ΔT_j) and cycle heating time (T_{on}), along with constant parameters $A, \beta_1, \beta_2, \beta_3$.

$$N_f = A \cdot \Delta T_j^{\beta_1} \cdot exp\left(\frac{\beta_2}{T_j + 273}\right) \cdot T_{on}^{\beta_3} \tag{3.7}$$

The thermal cycles were organized by the rainflow counting algorithm and these are fed to the lifetime model to calculate the number of cycles to failure (N_f) for a specific combination of thermal parameters. Once this is done, the thermal cycles occurred (n_i) and the number of cycles to failure (N_{fi}) are compared with the use

Table 3.2: Constant parameters of the Bayerer's lifetime model

Parameter	Value
A	$3.43x10^{14}$
β_1	-4.416
β_2	-0.716
β_3	-0.761

of the Miner's rule (3.8) to obtain the life consumption (LC) for the given mission profile. When $LC \geq 1$ the end of life is reached [45].

$$LC = \sum_i \frac{n_i}{N_{fi}} \tag{3.8}$$

3.6 Monte Carlo reliability assessment

The lifetime model described above could be defined as an ideal model, where all IGBT devices would fail at the same time. The parameters in the Bayerer's lifetime model [13] consider uncertainties in the parameters. These uncertainties are going to be evaluated in this work with the use of Monte Carlo simulation. Such a model gives a probabilistic estimation of the lifetime of the system, considering parameters variations in the lifetime model. The parameter variation of the Bayerer's lifetime model is done with a normal Probability Density Function (PDF).

Moreover, the PV system is going to be evaluated for daily mission profiles in the case of the Temperature-controlled MPPT algorithm (Chapter 5.1) and for a yearly mission profile in the case of the Maximum-temperature-limited MPPT algorithm (Chapter 5.2). The daily mission profiles represent just individual cases that can vary through the year, for example they can be affected by seasonal changes. However, the yearly mission profile better represents the behaviour of the system in the long term. For this reason, the Monte Carlo simulation is going to be applied just for the yearly mission profile assessment.

The Monte Carlo simulation is used in reliability analysis to express the reliability of the system with a probabilistic solution instead of a fixed value. The Monte Carlo assessment consists of a repeated evaluation of the model using different values of

the distributed parameters [16]. For this work 10,000 repetitions are going to be implemented for the normally distributed parameters β_1, β_2 and β_3 given in [13], which are part of the equation (3.7).

The yearly mission profile is composed of a large amount of random thermal fluctuations that would make the Monte Carlo analysis difficult to execute. For this reason, the annual accumulated damage for one year is used as a reference to apply the Monte Carlo simulation. It is necessary to calculate a specific set of thermal parameters $(T_j, \Delta T_j, T_{on})$ that would inflict the same damage during a year as the annual accumulated damage. This set of parameters is known as equivalent static values $(T'_j, \Delta T'_j, T'_{on})$. There are many different combinations of parameters that can provide the equivalent annual accumulated damage. To lower the degree of freedom T'_{on} and T'_j are fixed [22]. T'_{on} is 0.083, which matches with the grid frequency $(60Hz)$. The static junction temperature T'_j is obtained from the average junction temperature during the year mission profile. The temperature differential static value $(\Delta T'_j)$ needs to be mathematically calculated.

To calculate the $\Delta T'_j$, it is necessary to know the life consumption (LC) of the system for one-year mission profile and the number of thermal cycles occurred (n) during that year. The number of thermal cycles occurred will be obtained from the multiplication of 365 days, 24 hours, 60 minutes, 60 seconds and 60 Hertz. Then the equation 3.7 is substitute in equation 3.8.

$$LC = \frac{n}{A \cdot \Delta T_j^{\beta_1} \cdot exp\left(\frac{\beta_2}{T_j+273}\right) \cdot T_{on}^{\beta_3}} \tag{3.9}$$

From the above equation the variable to be calculated is $\Delta T'_j$, thus this variable needs to be isolated [22].

$$\Delta T'_j = \sqrt[\beta_1]{\frac{n}{A \cdot exp\left(\frac{\beta_2}{T_j+273}\right) \cdot T_{on}^{\beta_3} \cdot LC}} \tag{3.10}$$

With the obtaining of the equivalent static values $(T'_j, \Delta T'_j, T'_{on})$ it is possible to easily apply the Monte Carlo method to estimate the reliability of a PV system.

3.6.1 Summary

With the application of the lifetime evaluation method described in this chapter, it is possible to calculate the reliability and lifetime consumption of a PV system under a specific mission profile. This lifetime evaluation presents and provides a route to compare the reliability of PV systems, which can be useful in comparing techniques to improve the lifetime. In this work the lifetime evaluation is going to be used in the assessment and comparison of identical PV systems which are controlled with normal and modified MPPT control methods. In the following chapter these modified MPPT methods will be presented and explained. In Chapter 5 the lifetime evaluation method explained will be applied and the results will be discussed in detail.

Chapter 4

Proposed MPPT algorithms

The lifetime of power electronic IGBTs can be estimated based on the temperature changes experienced by the device for the mission profile. Thus, with the regulation and reduction of thermal stresses, the reliability and lifetime of power electronics can be enhanced. The thermal management of power converters can be free of extra investment with adjustment in the control stage. In this work two algorithms for thermal management of PV power converter are presented: one algorithm aims to limit the junction temperature change rate during dynamic irradiance conditions, while the purpose of the second algorithm is to decrease the power generation limiting the maximum junction temperature.

The modified maximum power point tracking (MPPT) algorithms are applied to control the boost stage of a two-stage PV converter. For boost converters, the output voltage (V_{Out}) is affected by the input voltage (V_{In}) in relation with the duty cycle as seen in equation (4.1) [46]. With the reduction of the duty cycle, the output voltage is reduced and the output power is limited, limiting the temperature rise of the devices.

$$V_{out} = \frac{V_{in}}{1 - D} \tag{4.1}$$

There are several control strategies to find the maximum power point (MPP) in a PV system, with Perturb and observe (P&O) methods being among the best ranked due to the low implementation costs as they do not require additional elements in the system [31]. A normal P&O algorithm just needs to measure the PV voltage

(V) and current (I), based on the power calculated the algorithm change the duty cycle, always searching for the MPP. A flow diagram of this algorithm can be seen in Fig. 4.1, where at each iteration the current and voltage are measured and the power (P) calculated. The present power (P_k) is compared with the previous one (P_{k-1}), if the power and the voltage increased ($dP > 0$ and $dV > 0$), then the duty cycle is reduced ($D = D - \Delta D$). If the power increased but the voltage was reduced ($dP > 0$ and $dV < 0$), the duty cycle is increase ($D = D + \Delta D$). Otherwise, in the case that the power is reduced, and the voltage is lower than the previous one ($dP < 0$ and $dV < 0$), the duty cycle will be reduced ($D = D - \Delta D$) and if the power is lower than the previous one and the voltage is higher ($dP < 0$ and $dV > 0$), the duty cycle will be increased ($D = D + \Delta D$).

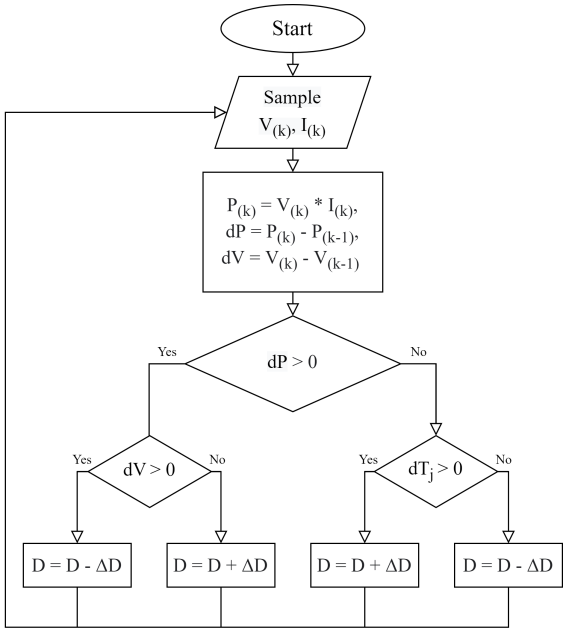

Figure 4.1: Flow diagram of a normal MPPT algorithm.

In the next sections, the TC and MTL MPPT algorithms will be explained, both algorithms are modifications of a normal P&O MPPT algorithm.

4.1 Temperature-controlled MPPT algorithm

In PV applications the solar irradiance and ambient temperature are the main factors that influence temperature changes. Moreover, solar irradiance is especially

dynamic during fast-changing cloud conditions. With continuous variations of solar irradiance, the temperature of IGBT switches varies constantly, which in turn leads to higher thermal stress and a lower lifetime period. To overcome this issue a temperature-controlled (TC) MPPT algorithm has been developed, the algorithm was developed with the idea presented in [29] as a reference, with the improvement of reducing the necessary steps in the algorithm which makes it faster. Moreover, the TC MPPT algorithm is used to evaluate lifetime improvement of PV system under dynamic cloud conditions. The algorithm is intended to limit the speed of temperature changes caused by the variations of solar irradiation during cloudy days, thus reducing the damage received.

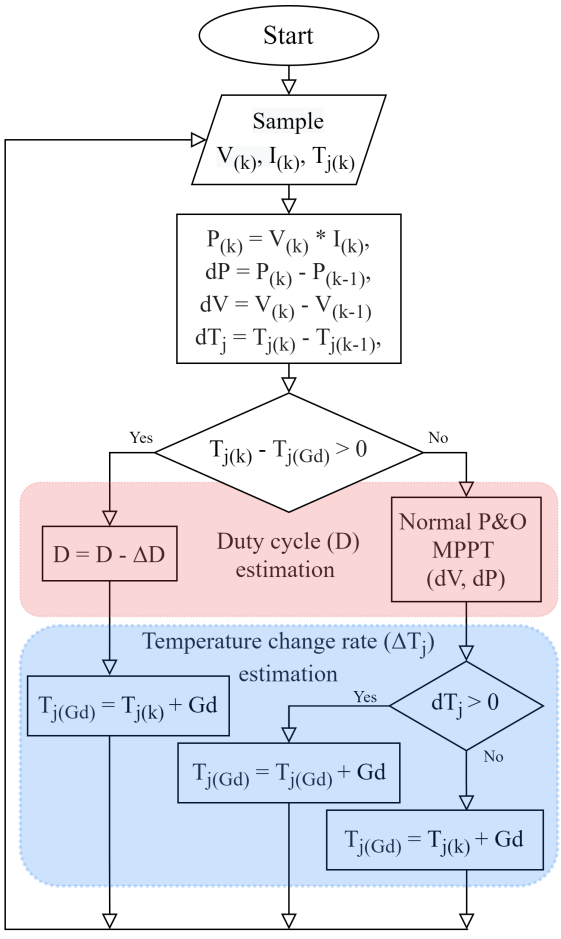

Figure 4.2: Flow diagram of the temperature-controlled MPPT algorithm.

With the application of the TC MPPT algorithm thermal parameters such as mean junction temperature (T_j) and temperature differential (ΔT_j) are reduced. The damage received by IGBT devices is highly dependent on thermal parameters,

therefore we can expect considerable damage reductions with small temperature reductions based on the equation 3.7. Despite the reduction in damage received, it is important to remark that the algorithm also has an impact on the energy generated by the system. The algorithm works by controlling the duty cycle depending on the temperature changes that occurred in the IGBT devices which in turn make the maximum power point tracking slower, thus generating less energy. For this reason, is important to evaluate to what extent the lifetime improvement outweighs the energy generation reduction.

The TC MPPT works by regulating the duty cycle (D). The difference with a normal MPPT algorithm is that the proposed algorithm is able to limit the temperature change rate to a preset value. In order to control the temperature change rate, the algorithm requires the temperature of the device to be calculated. The first step in the algorithm is to sample the current junction temperature (T_j) in the switching device, along with the voltage (V) and electric current (I) of the PV array. Then, from the sampled elements the power (P) is calculated. From the previous and current values the differential of power (dP), voltage (dV) and temperature (dV) are obtained. Next, if T_j does not surpass the temperature change rate limit ($T_{j(Gd)}$), the duty cycle is reduced and the new $T_{j(Gd)}$ is the current T_j plus the fraction of gradient Gd. Otherwise, a normal MPPT algorithm is applied to adjust the duty cycle and based on the temperature differential (dT_j), the temperature change rate limit ($T_{j(Gd)}$) is calculated. If the temperature is increasing ($dT_j > 0$), the new $T_{j(Gd)}$ is going to be the previous $T_{j(Gd)}$ plus the fraction of gradient (Gd), otherwise the new $T_{j(Gd)}$ is the current junction temperature (T_j) plus Gd. The gradient is the temperature change rate allowed, the fraction of gradient (Gd) at each iteration is obtained by multiplying the gradient and the sample time (T_s) as seen in (4.2).

$$Gd = Gradient \times T_s \tag{4.2}$$

4.2 Maximum-Temperature-limited MPPT algorithm

In this section a second MPPT algorithm is going to be presented, this algorithm will be named as maximum-temperature-limited (MTL) MPPT algorithm. This algorithm has the objective of limit the maximum junction temperature ($T_{j(max)}$) that an IGBT device can reach. The MTL algorithm is also based on the MPPT control algorithm presented in [29]. One application of such an algorithm is to ensure that the device never reaches the maximum operating temperature that would cause immediate failure. Another application of the MTL MPPT algorithm presented and analysed in this work is the power reduction for lifetime improvement, this feature can be use to harvest the maximum energy possible during days with high irradiance and ambient temperature values and will be further explained in this section. With the power reduction of the system, power losses and junction temperature of IGBTs are reduced as well. As commented before, the reduction of thermal parameters in switching devices leads to damage reduction based on equation 3.7.

The MTL MPPT algorithm evaluated in this work can be compared with the power reduction strategy presented in [27]. Although both strategies are able to reduce the output power of PV systems, the proposed algorithm has the advantage of reducing the output power just when necessary. Based on an analysis that considers the control of the output power of the system together with the ambient temperature, the proposed algorithm can reduce the output power just when a junction temperature limit has trespassed. While the strategy proposed in [27] is controlled based on the output power of the system, the MTL MPPT algorithm is able to let the system work at full capacity during high irradiance level conditions (high output power) as long as the ambient temperature is low enough to allow the heat dissipation to maintain the junction temperature below the temperature limit.

The temperature of the IGBT devices increases with higher losses produced by the PV system during greater irradiance levels. Another factor that influences the junction temperature level is the ambient temperature, which has a direct impact on the junction temperature, and higher ambient temperatures result in higher junction

temperatures. For winter months, both the ambient temperature and irradiance levels are low, the damage received by the PV system is low and the MTL MPPT algorithm does not affect the normal performance of the PV system. During the summer months, when the ambient temperature and irradiance levels increase, the damage caused to the PV system is greater, this is when the MTL MPPT algorithm limits the energy production to reduce the damage impact on the switching devices.

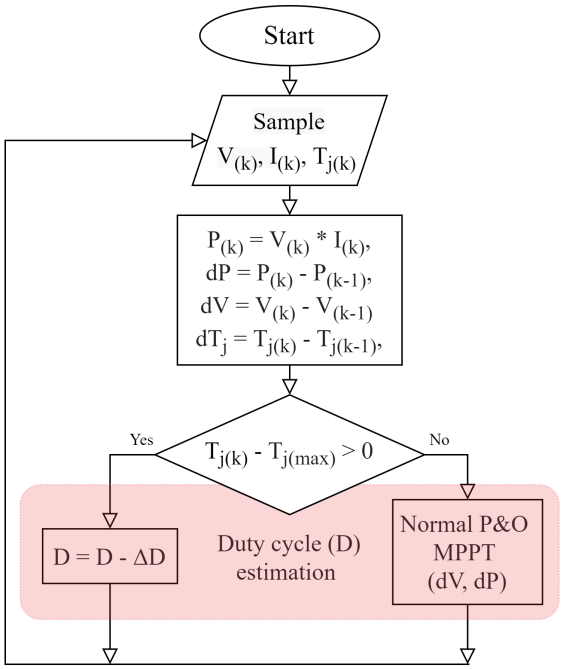

Figure 4.3: Flow diagram of the maximum-temperature-limited MPPT algorithm.

In this paragraph, the process of the MTL MPPT algorithm will be described. This algorithm adjusts the duty cycle of the boost converter every time the junction temperature of a switching device cross a certain temperature limit. As can be seen in Fig. 4.3, it is necessary to sample the voltage (V_k) and current (I_k) of the system to apply the normal MPPT algorithm when necessary. It also requires to sample the junction temperature ($T_{j(k)}$) of a switching device to enable the control the maximum temperature. After the sampling is done, the current power as well as the power (dP) and voltage (dV) differentials are calculated. The next step is to compare the current junction temperature ($T_{j(k)}$) with the maximum temperature allowed ($T_{j(max)}$). If the junction temperature is above the limit, the duty cycle is reduced, otherwise, a normal MPPT algorithm is applied to adjust the duty cycle.

Chapter 5

Simulations and results

A PV system has been designed to perform the analysis of the lifetime of IGBTs (See Fig. 5.1). The system is composed of a PV array and a two-stage PV inverter connected to the grid as described in Chapter 3.1. This electrical model designed in Matlab Simulink is identical for the application of both MPPT algorithms mentioned in Chapter 4.

The PV array of the system is composed of 250 Watts PV solar panels from Trina manufacturer [47], the parameters of the solar panel can be seen in Table 5.1. The PV array is made up of a total of 40 solar panels and a rated power of 10kW. The solar panels are arranged in 10 series-connected solar panels called strings, and 4 parallel-connected strings.

Table 5.1: Electrical parameters of the 250W Trina Solar PV Panel at Standard Test Conditions (STC) values

Description	Parameter	Value
Power at maximum power point	Pmp	250 W
Open circuit voltage	Voc	37.6 V
Voltage at maximum power point	Vmp	31.0 V
Short-circuit current	Isc	8.85 A
Current at maximum power point	Imp	8.06 A

The first stage of the inverter is controlled by a perturb and observe (P&O) MPPT algorithm, it is important to notice that the modified MPPT algorithms are influenced by the temperature extracted from a switching device. For this reason, it is necessary to build a block which is in charge of calculating the power losses and the

junction temperature, and to alter the normal MPPT algorithm with a temperature control block. The second stage control remains unchanged. The IGBT devices used in the system are IKW50N60H3 from Infineon manufacturer [48], one device for the boost stage and four devices for the H-bridge stage. The parameters for the rest of the elements of the system are listed in Table 5.2, a relatively low switching frequency (3 kHz) has been set to show that even with low switching frequency and therefore lower thermal stress, the modified algorithm is able to improve the reliability of the PV system.

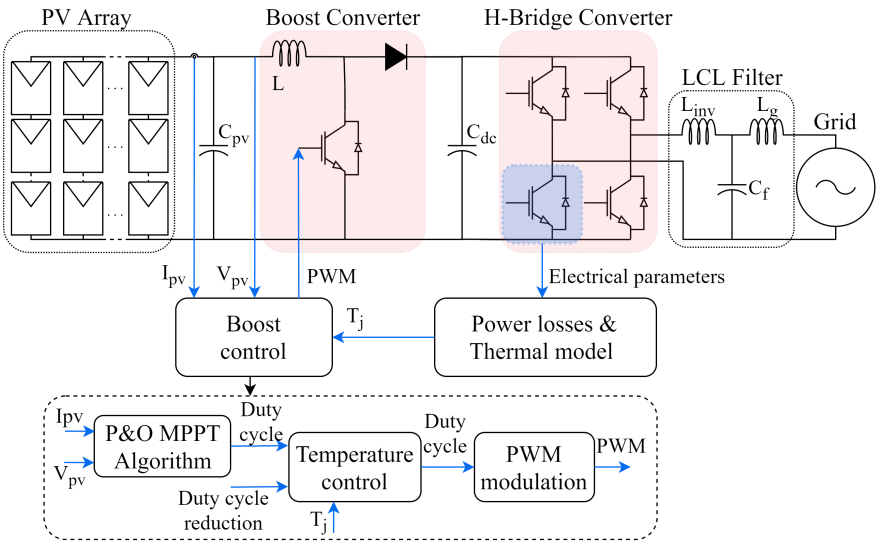

Figure 5.1: Electric diagram of the PV system with temperature control.

For the power losses calculation (Chapter 3.2), it is necessary to include in the model the on-state resistance of IGBT (R_{on}) and diode (R_D). This as the conduction losses for both devices are dependent on the on-state resistance. To obtain the on-state resistance of IGBTs the "Typical output characteristics" graph is used at the highest T_j as it represents the worst-case scenario [39], we use the 175°C graph in this case.

From Fig. 5.2a the R_{on} can be calculated. The graph shows the relationship of Collector to emitter voltage (V_{ce}) and Collector current (I_c) with respect of different Gate to emitter voltages (V_{ge}), as Infineon uses 15 volts in V_{GE} when testing, that is the curve that is going to be used. To calculate the R_{on} it is necessary to draw a line between two points in the slope and calculate the inverse slope as seen in equation (5.1).

Table 5.2: Electrical parameters of the 2-stage 10kW PV converter

Description	Parameter	Value
Two-stage PV converter		
Rated power		10 kW
Grid frequency		60 Hz
Grid voltage	(RMS)	240 V
Switching frequency	f_{sw}	3 kHz
Boost converter		
Inductor	L	$1.3mH$
PV capacitor	Cpv	$1000\mu F$
DC-link capacitor	Cdc	$1500\mu F$
LCL filter		
Inverter side inductor	Linv	$3.6mH$
Grid side inductor	Lg	$8.6mH$
Capacitor	Cf	$9.5\mu F$

$$R_{on} = \frac{V_{ce2} - V_{ce1}}{I_{c2} - I_{c1}} = \frac{4V - 3V}{138A - 93A} = \frac{1V}{45A} = 0.0222\Omega \tag{5.1}$$

A similar process is applied to the diode from the "Typical diode forward current as a function of forward voltage" chart (See Fig. 5.2b The diode on-state resistance (R_D) is obtained with the equation:

$$R_D = \frac{V_{D2} - V_{D1}}{I_{D2} - I_{D1}} = \frac{2V - 1.5V}{60A - 32A} = \frac{0.5V}{28A} = 0.0179\Omega \tag{5.2}$$

The rest of the parameters necessary for power losses estimation can be extracted directly from the datasheet at the highest T_j to represent the worst-case scenario. These parameters can be seen in Table 5.3.

Table 5.3: Parameters for the power losses calculation

Description	Parameter	Value
IGBT		
On-state resistance	R_{on}	0.0222Ω
Turn-on energy	E_{on}	$1.42mJ$
Turn-off energy	E_{off}	$1.13mJ$
Diode		
On-state resistance	R_D	0.0179Ω
Reverse recovery energy	E_{rec}	$0.96mJ$

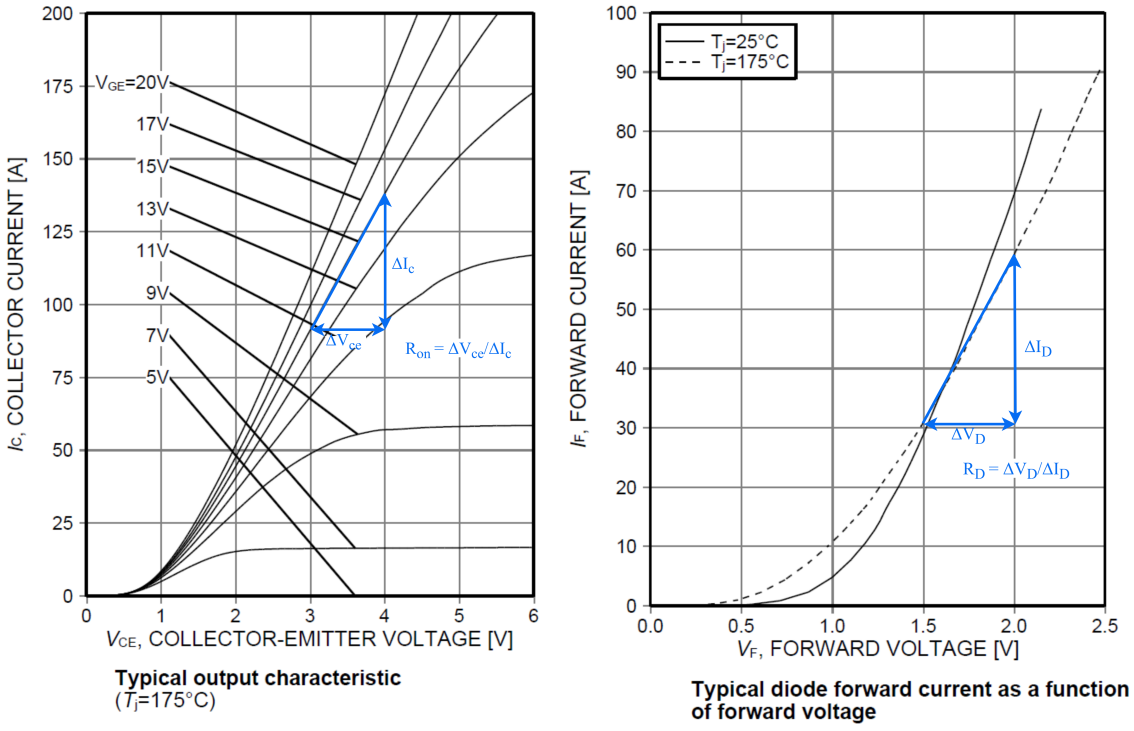

(a) IGBT

(b) Diode

Figure 5.2: On-state resistance calculation *Figures extracted from [48]

As discussed in Chapter 3.3 a Foster model was selected as the thermal equivalent model used in this work. Such model is implemented to assess the power losses and can be seen in Fig. 5.3, where the individual layers of switch and diode are connected in parallel to represented the thermal relationship between elements [43]. Each the IGBT and diode have an individual current source to represent the power losses, a certain number (n) of individual RC elements for the junction to case section $(j - c)$ [42]. Afterwards, both layers merge in the case to heat-sink $(c - h)$ section, the model continues to the heat-sink to ambient $(h - a)$ section and finally, a DC source takes place to represent the ambient temperature. The parameters of the Foster model are listed in Table 5.4.

The capacitance values are not provided directly, so it is necessary to calculate them with:

$$C_n = \tau_n / R_n \tag{5.3}$$

Where C_n is the thermal capacitance value, τ_n is the thermal time constant and

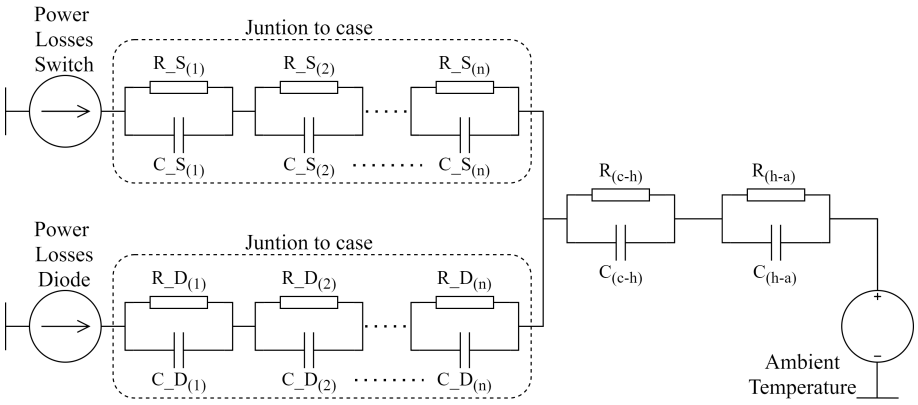

Figure 5.3: Foster diagram of the PV converter

Table 5.4: IGBT and diode thermal parameters for the Foster thermal model

Impedance		$Z_{th(j-c)}$					$Z_{th(c-h)}$
	n	1	2	3	4	5	
IGBT	R_n (K/W)	7.0e-3	0.037	0.092	0.130	0.183	0.7
	τ_n (s)	4.4e-5	1.0e-4	7.2e-4	8.3e-3	0.074	0.25
Diode	R_n (K/W)	0.049	0.225	0.313	0.268	0.195	0.7
	τ_n (s)	7.5e-6	2.2e-4	2.3e-3	0.015	0.107	0.25

R_n is the thermal resistance.

5.1 Application of the temperature-controlled MPPT algorithm

In this section the modified MPPT algorithm presented in Chapter 4.1 will be evaluated. The TC MPPT algorithm is able to reduce the temperature change rate of IGBT device during operation. For example, when a cloud is passing over a PV system, the irradiance levels will change, causing a variation in the output power and therefore a change in the temperature of the devices. These thermal variations are the cause of damage that reduce the lifetime of IGBT devices. The TC MPPT algorithm is capable of reducing the thermal stress experienced during this period, therefore improving the lifetime of the PV system. For the correct evaluation of the impact that the modified algorithm has, it is necessary to calculate the lifetime improvement. To do so, a lifetime evaluation approach will be presented, this method

is adapted from the one shown in [24]. The flow diagram as seen in Fig. 5.4 shows the process of the lifetime estimation process, which is going to be further explained in the rest of the section.

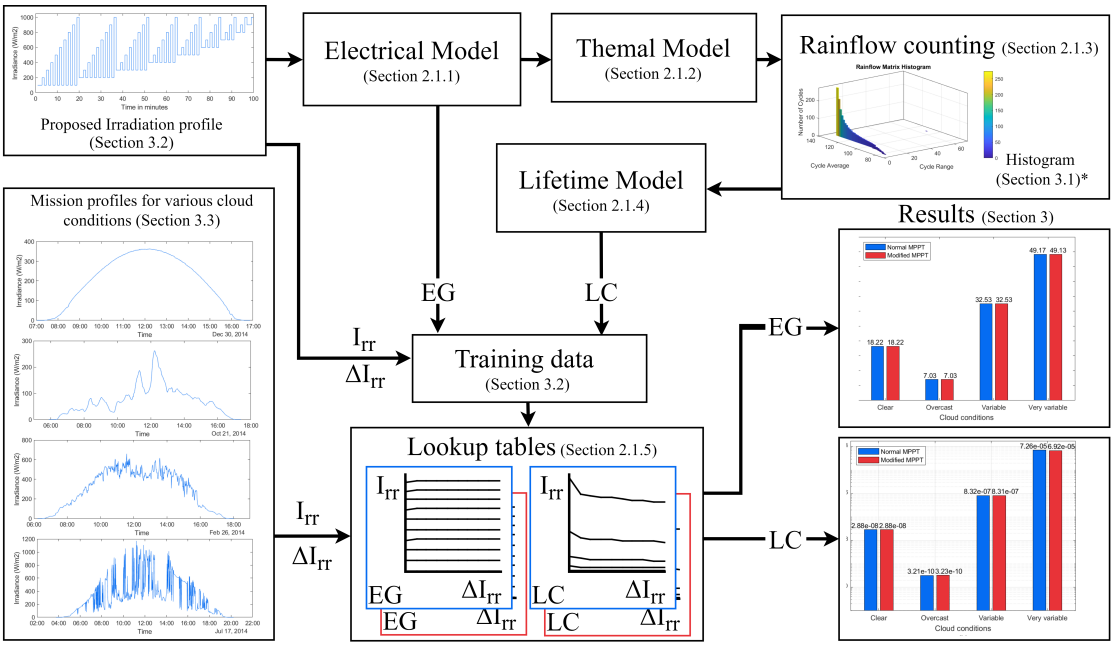

Figure 5.4: Flow diagram of the proposed method to estimate the life consumption and energy generated by the system. I_{rr} is the current irradiance level, ΔI_{rr} is the differential of the current and previous irradiance level, EG is the energy generated, and LC is the life consumption

5.1.1 Temperature change rate limitation

The TC MPPT algorithm is tested in order to prove it is functional. The temperature change rate selected for this work is $3°C/S$. To test the algorithm a solar irradiance step change with short rise time from $100W/m^2$ to $1000W/m^2$ and ambient temperature of $25°C$ is applied to the PV system in Simulink, the comparison of the effect in temperature of both normal and TC MPPT algorithm can be seen in Fig. 5.5.

The application of the algorithm shows an effect in both the mean junction temperature (Fig. 5.5a) and the temperature differential (Fig. 5.5b). With the application of the TC MPPT algorithm the temperature variations of IGBTs are altered, causing the mean junction temperature (T_J) to rise at a lower speed and temperature differential (ΔT_j) is reduced, which has a positive effect in the lifetime

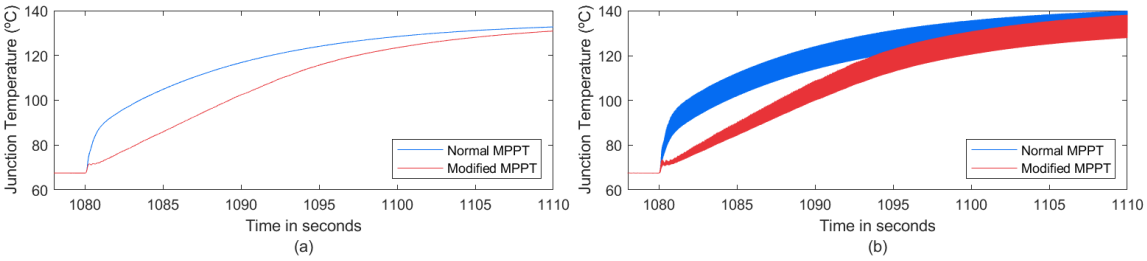

(a) Mean junction temperature

(b) Junction temperature differential

Figure 5.5: Mean junction temperature and temperature differential

of IGBT devices, this as lower thermal parameters have a lower impact on lifetime consumption, which have been previously discussed.

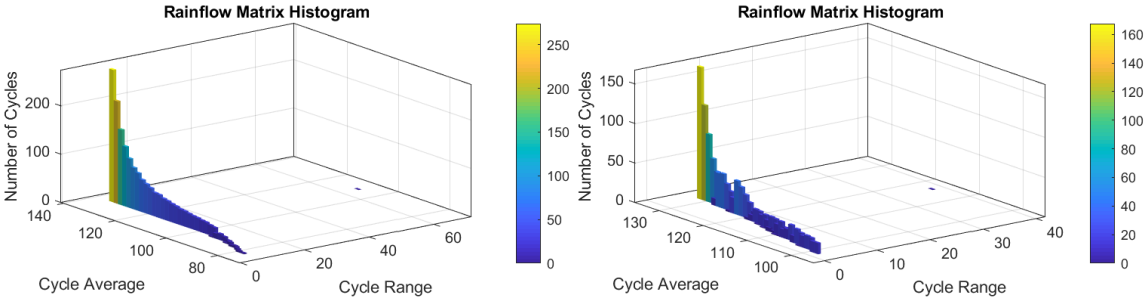

(a) Normal MPPT

(b) Temperature-controlled MPPT

Figure 5.6: Application of the rainflow counting algorithm

To further compare the effect of the algorithm in the temperature of IGBTs the rainflow counting of both MPPT algorithms can be seen in Fig. 5.6. The histograms were obtained by applying the process described in Chapter 3.4 to the temperature profiles. The effect of the modified algorithm in the temperature cycles of IGBTs is visible, with a reduction of the cycle average (T_j) and cycle range (ΔT_j). The T_j is redistributed in lower values which can be seen in the number of cycle per bin, the ΔT_j values are also reduced.

5.1.2 Irradiance mission profile (Training)

The simulations needed to evaluate the life consumption of complete daily mission profiles would be really time-consuming which make them unfeasible. To overcome this problem, Lookup Tables (LUTs) are used in this work to reduce computation time. To apply LUTs it is necessary to obtain a base data set from the simulations of the PV system.

In order to obtain a base data set for the LUTs and test the effectiveness of the proposed algorithm, it is necessary to create a solar irradiance profile and compare the performance of both normal and modified MPPT algorithms. The proposed solar irradiance profile (Fig. 5.7) is made up of one-minute irradiance steps to match with the high-resolution cloud conditions irradiance data sets which have a sample time of one minute between samples. These irradiance mission profiles are described in Chapter 5.1.3. Moreover, small-scale irradiance fluctuations do not have a considerable impact on PV system [11]. Large-scale irradiance fluctuations ($\Delta Irra > 100W/m^2$) need to be considered, for this reason the step changes in the proposed irradiation profile (Fig. 5.7) have at least a irradiance differential of $100W/m^2$. The irradiance values are all multiples of $100W/m^2$ in a range from 100 to 1000, the result of all other values are calculated by interpolation and extrapolation of the reference values. The mission profile has a total length of 100 minutes in order to cover all the combinations of irradiance changes.

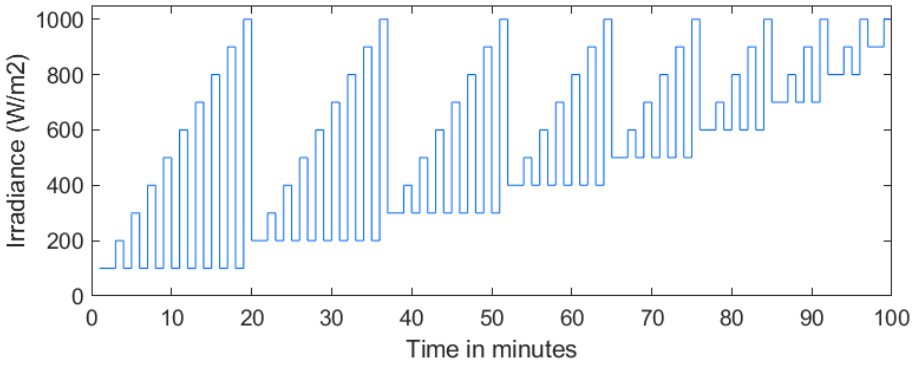

Figure 5.7: Proposed solar irradiance profile

The explained irradiance mission profile and an ambient temperature of $25°C$ are implemented to the previously described 10kW PV system in Simulink. It is necessary to calculate the junction temperature while the system is operating, for the normal MPPT algorithm the temperature could be evaluated after simulation, but the TC MPPT requires real-time calculation of the temperature. For this reason, the power losses are calculated during the simulation, then used by the Foster model to obtain the temperature and then used as an input for the MPPT algorithm used to control the temperature change rate. After simulation of the proposed mission profile for both normal and TC MPPT algorithms, the results are used to create

LUTs that will be later used to evaluate the performance of the PV systems for longer mission profiles.

The temperature profiles obtained for both algorithms are first separated into individual one-minute profiles and labelled based on the previous and current irradiance levels. Afterwards, the individual profiles are processed in Matlab to obtain the peaks and valleys as described in Chapter 3.4, and then the rainflow function is applied to organize the random temperature cycles (See Chapter 5.1.1). Next, the lifetime model is applied to estimate the life consumption of the switch device during the given irradiance profile and finally, Miner's rule is applied to sum the life consumption of all the individual cycles. This process is repeated to all the individual one-minute profiles.

Once the lifetime evaluation of the proposed mission profile is done, we proceed to compare the results of life consumption and energy generated for both algorithms. The energy generation for both the normal and TC MPPT algorithms can be seen in Fig. 5.8a and the life consumption in Fig. 5.8b. The application of the TC MPPT algorithm has an observable effect. The energy generated was reduced 0.35% which is a small amount compared with the life consumption reduction which accounts for 12.24%. The comparison of energy generated and life consumption of both algorithms for the proposed mission profiles validates the effectiveness of the algorithm (See Table 5.5).

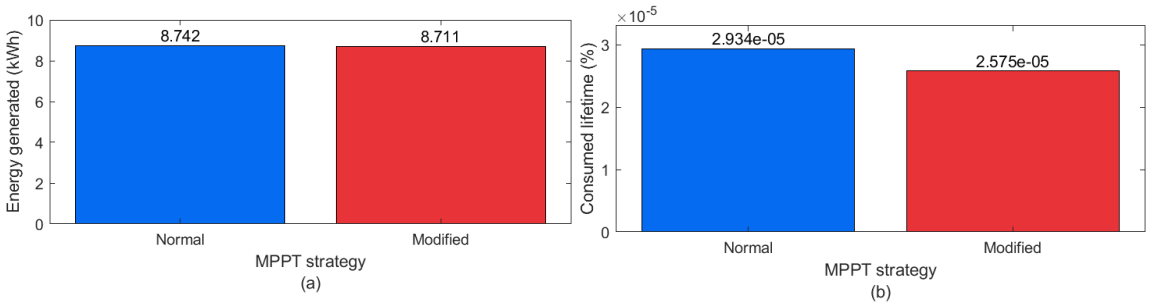

(a) Energy generated

(b) Life consumption

Figure 5.8: Comparison of the energy generated and life consumption with the proposed mission profile

Now that the efficacy of the TC algorithm has been validated, we need to analyse the effect that the modified algorithm will have for the cloud conditions irradiance profiles. However, it is necessary to first set up and verify the LUTs. The LUTs

Table 5.5: Comparison of normal and the controlled MPPT algorithm effects on the energy generated and the life consumption of the converter under the proposed mission profile. EG is the energy generated and LC is the life consumption.

	MPPT strategy	Values
EG(kWh)	Normal	8.742
	Modified	8.711
LC(%)	Normal	2.934e-05
	Modified	2.575e-5

setup is done with help of the "2-D Lookup Table" block in Simulink.

There are two sets of two LUTs each, giving a total of four LUTs, the first set is applied to estimate the energy generated, one LUT for the normal MPPT algorithm and the other for the TC MPPT algorithm. The second set is the same as the first but to estimate the life consumption instead. The inputs of the LUTs are the previous and current irradiance level. The LUTs dimension is 10 by 10, one coordinate of the LUTs is the current irradiance level and the other coordinate is for the previous irradiance level and both coordinates represent the values from $100W/m^2$ to $1000W/m^2$ in $100W/m^2$ steps. When an input combination of values match with the LUTs coordinates, the output value is obtained from the intersection of the given row and column. If the input does not match the coordinate but is within the range, the result is mathematically approximate by interpolation. If the input does not match the coordinate and it is out of range, the result is mathematically approximate by extrapolation.

For the verification of the LUT performance, a solar irradiance mission profile was designed (See Fig. 5.9) to evaluate the confidence level. The mission profile is composed of 20 minutes of solar irradiance. The PV system is tested with the mentioned mission profile. The irradiance profile is also processed by the LUTs. The energy generated (Fig. 5.10a) and life consumption (Fig. 5.10b) is obtained from simulation results and LUT estimation. The confidence level of the LUT to estimate the energy generated is 99.9%, while for the life consumption, the LUTs confidence level is 95.34%.

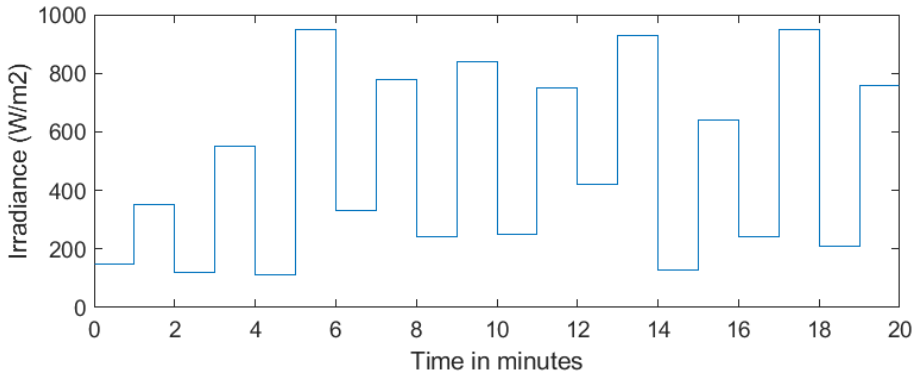

Figure 5.9: Irradiance profile to test the performance of the LUTs

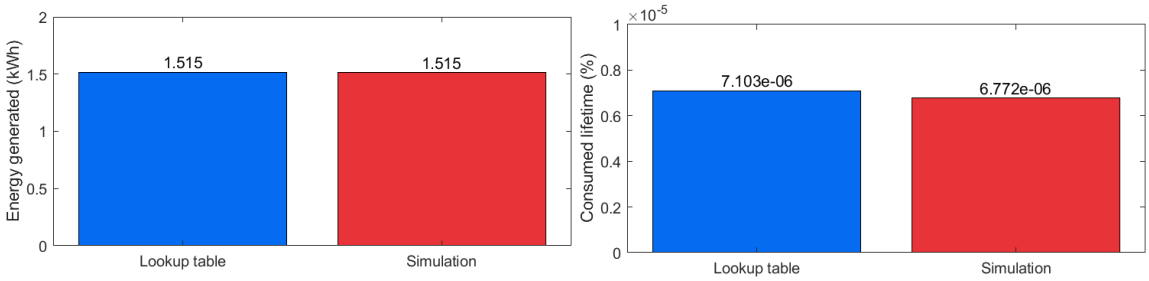

(a) Energy generated

(b) Life consumption

Figure 5.10: Example of the energy generated and life consumption obtained from the LUTS and Simulation for the normal MPPT algorithm

5.1.3 Simulation of Irradiance Mission Profiles

Now that the effectiveness of the TC MPPT algorithm has been validated it can be applied to the daily irradiance mission profiles. However, as commented before, the simulation of such mission profiles would be impractical for the amount of simulation time required. With the set-up and verification of the LUT, it is possible to accurately evaluate the life consumption and energy generated by the PV system for the daily irradiance mission profiles. To this end, four different irradiance data sets are used to feed the LUTs and the generated energy and life consumption of the IGBT devices are determined for each of them.

The data sets used in this work are from the province of Quebec, Canada [49]. To obtain the high-resolution solar irradiance data sets, very precise irradiance sensors were used to allow the millisecond sample rate. To reduce the size of the data sets, recording of data is limited to a resolution sample rate of 1 second if at least $5W/m^2$ change in the data is observed, otherwise the irradiance is recorded every minute [49]. The data sets represent four different types of cloud conditions: clear

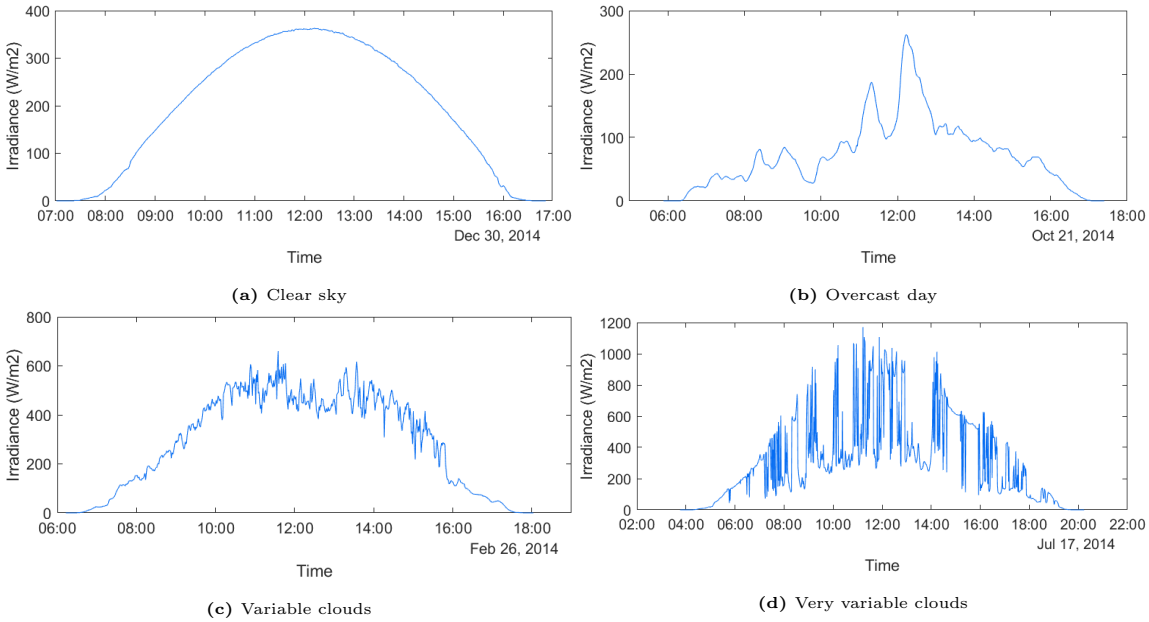

(a) Clear sky

(b) Overcast day

(c) Variable clouds

(d) Very variable clouds

Figure 5.11: Irradiance profiles during days for clear sky (a), overcast (b), variable (c) and very variable (d) cloud conditions in the province of Quebec, Canada.

sky, overcast, variable and very variable shown in Fig. 5.11. To have regular intervals that allow consistent comparison of data between different cloud conditions, just the one-minute data samples are used in this work.

To apply the LUTs, the daily solar irradiance mission profiles described above are fed to the LUTs in the Simulink environment. The performance of the normal MPPT algorithm and the TC MPPT algorithms are compared. In Fig. 5.12, the accumulated life consumption of the four different mission profiles can be seen. For days with clear sky, overcast and variable cloud conditions the life consumption is the same as the effect of the algorithm are negligible. For days with very variable cloud conditions, the TC MPPT algorithm managed to reduced the life consumption (See Fig. 5.12d).

The energy generated and life consumption for the four different cloud conditions can be seen in Fig. 5.13. For days with clear sky, overcast or variable cloud conditions the energy generated and life consumption difference is negligible. This was expected for clear sky days and overcast conditions as the irradiance changes are slow. However, the TC MPPT algorithm did not have an effect in days with variable cloud conditions although there are constant changes in irradiance and this will be explained in the next subsection. For days with very variable cloud conditions, the

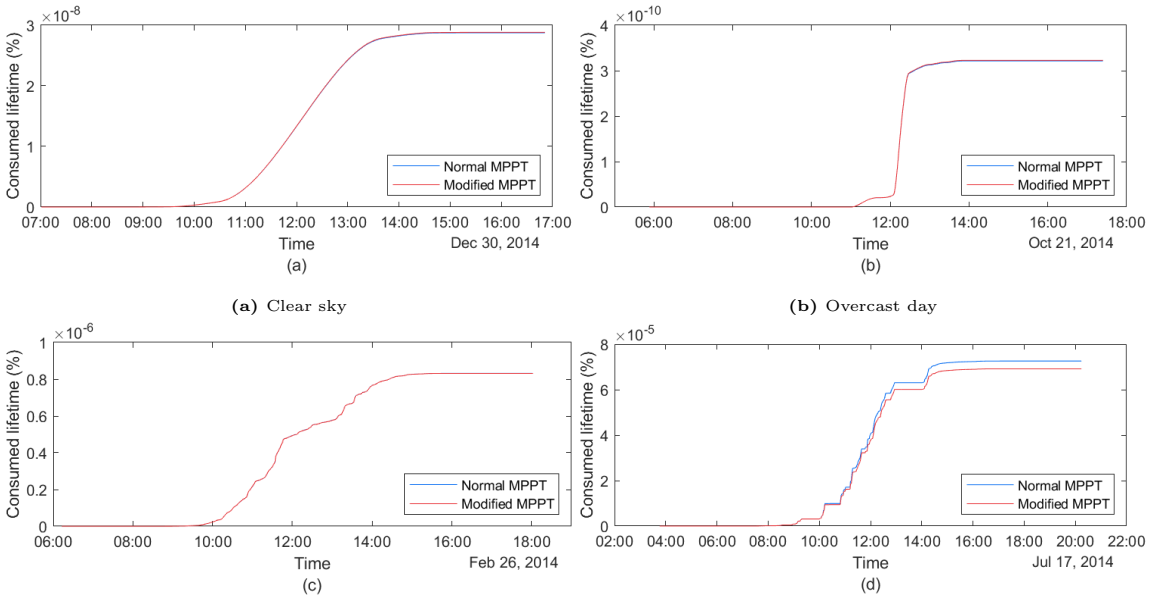

(a) Clear sky

(b) Overcast day

(c) Variable clouds

(d) Very variable clouds

Figure 5.12: Accumulated life consumption of the PV inverter under one day mission profile for clear sky (a), overcast (b), variable (c) and very variable (d) cloud conditions

algorithm was effective as expected, the lifetime consumption was reduced by 4.68% with the application of the algorithm, with a reduction of the energy generated of 0.08%, which show a great improvement in lifetime and reliability at a small energy cost (See Table 5.6).

Table 5.6: Comparison of normal and the controlled MPPT algorithm effects on the energy generated and the life consumption of the converter under different cloud conditions. EG is the energy generated and LC is the life consumption.

	MPPT strategy	Values			
		Clear sky	Overcast	Variable	Very variable
EG(kWh)	Normal	18.22	7.03	32.53	49.17
	Modified	18.22	7.03	32.53	49.13
LC(%)	Normal	2.88e-8	3.21e-10	8.32e-07	7.26e-05
	Modified	2.88e-09	3.23e-10	8.31e-07	6.92e-05

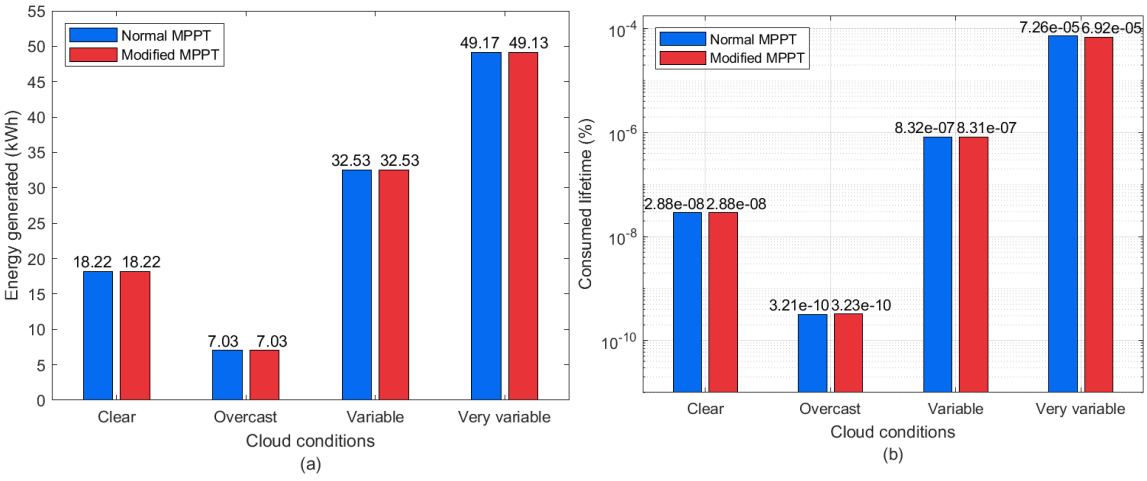

(a) Energy

(b) Damage

Figure 5.13: Comparison of the energy generated and life consumption during different cloud condition days

5.1.4 Limitations of the temperature-controlled MPPT algorithm

The previously explained MPPT algorithm proved to be effective in the reduction of damage received by IGBT switching devices in PV applications. The algorithm was able to improve the lifetime and reliability of a PV converter under very variable cloud conditions. This can be explained because the dynamic irradiance changes caused by the passing clouds leads to power and temperature variation in the IGBT devices, variations that the algorithm is able to control, reducing the temperature stress experienced by the IGBTs.

Although days with variable cloud conditions present dynamic irradiance changes, the algorithm did not achieve any perceivable effect improving the lifetime of IGBT devices. This can be explained due to the execution characteristics of the algorithm. The boost converter maximum power point (MPP) control takes into account the necessary output voltage (V_{out}) and alters the duty cycle (D) based on the available input voltage (V_{in}) to harvest the maximum energy possible. The relationship of parameters for boost converter can be seen in equation 4.1.

For days with clear sky conditions as there are not dynamic irradiance changes, the TC MPPT algorithm does not have any impact on the performance of the PV system, the algorithm behaves as expected. For days with overcast conditions, there are irradiance changes, but they are of small scale. Therefore, the application of the

modified algorithm does not present any appreciable effect on the system.

Apart from days with clear sky conditions where the irradiance changes are soft and follow an expected pattern, the rest irradiance profiles have the common characteristic of having unexpected irradiance changes during the day. Although these profiles have dynamic irradiance changes, the algorithm just had an effect for days with very variable cloud conditions. The difference between days with very variable cloud conditions with the other two dynamic irradiance profiles (variable and overcast cloud conditions), is that the irradiance changes during very variable cloud conditions are of large scale, while for the other two cloud conditions the irradiance changes are of small scale.

The maximum power point tracking as explained before, consist of a constant variation of the duty cycle using the input voltage as a reference. In Fig. 5.14 the maximum power point of the PV system at different irradiance levels can be seen, the pink circles represent those points. An irradiance change from $100W/m^2$ to $1000W/m^2$ causes a considerable shift in the input voltage, and the duty cycle variation is considerable as well. The same happen with changes from low irradiance levels (100 to $300W/m^2$). However, from irradiance levels of $400W/m^2$ and above, the input voltage of the system does not vary a lot, and the duty cycle change is not huge.

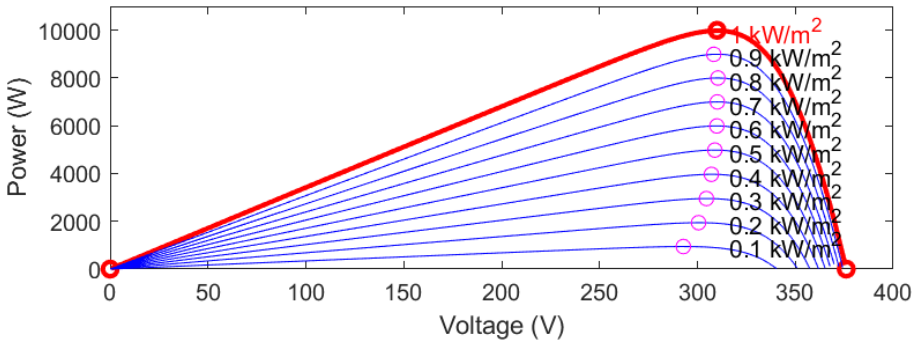

Figure 5.14: Irradiance profile to test the performance of the LUTs

Since the TC algorithm works by controlling the duty cycle change rate, having an appreciable change in the input voltage means that the algorithm has a substantial impact controlling the performance of the system, which is the case for very variable cloud conditions. Differently, for days with overcast and variable cloud

conditions, the irradiance changes are of small scale and the TC MPPT algorithm does not affect the performance of the PV system.

5.1.5 Summary

In this section the TC MPPT algorithm explained in Chapter 4.1 was implemented and evaluated. Moreover, a simulation time reduction was possible with the help of LUTs. With the application of the modified MPPT algorithm it was found that the lifetime of PV converters can be improved for dynamic irradiance conditions during very variable cloud conditions. For further research, the TC MPPT algorithm could be implemented to evaluate the lifetime impact for different converter topology that use MPP tracking. Also, the lifetime impact with different components or the evaluation of the PV systems in different locations with harsher environments. In the next section another modified MPPT algorithm will be evaluated. This algorithm similarly to the TC MPPT algorithm controls the temperature of switching devices to improve the lifetime of PV systems. The same lifetime evaluation approach as the one presented in this section will be use for the lifetime evaluation of the MTL MPPT algorithm.

5.2 Application of the maximum-temperature-limited MPPT algorithm

The MTL MPPT algorithm is a modified MPPT algorithm for the control of PV systems. The MTL is based on one protection feature of the algorithm presented in [29]. Originally the algorithm was intended to protect the IGBT devices against overheating. In this work, the algorithm founds further application, where the main goal is to improve the lifetime of PV systems. This is achieved by limiting the energy generation based on the solar irradiance together with the ambient temperature to reduce the damage on IGBT devices at the least energy reduction cost possible. The algorithm works by limiting the power of the PV system when the junction temperature of the IGBT switches reaches or cross a defined threshold. To achieve

the power reduction the algorithm modifies the duty cycle every time the junction temperature is above the desired level.

The MTL MPPT algorithm can be applied to ensure that the junction temperature never reaches critical levels, protecting the switching devices from breakdown. This can be useful for systems that have been over-designed to maximize energy production [14] where the IGBT devices are always on high-temperature stress levels. Another application of the MTL MPPT algorithm is to be used as a tool to limit energy production in order to improve the lifetime of a PV system. Lifetime improvement can be achieved because the damage that the IGBT devices experience due to temperature cycling is nonlinear and small reductions of temperature stress produce great reductions in the damage received.

The MTL MPPT algorithm works based on the junction temperature of the switching devices, which is affected by the solar irradiance and ambient temperature. This means that the limitation of the output power is done considering both parameters of the mission profile. Even if the solar irradiance levels are high (high energy production as well), the algorithm will not necessarily limit the power production if the junction temperature does not cross the temperature limit. The previous scenario can be possible during days with high irradiance levels but low ambient temperatures.

The simulation of a yearly mission profile would not be feasible due to the amount of time that would be necessary to process it. Therefore a similar approach for the lifetime evaluation as the one presented in the previous section (5.1.2) will be implemented, with the difference of a Monte Carlo reliability estimation for the case of this modified MPPT algorithm as explained in Chapter 3.6. This approach reduces the long time necessary for the simulation needed for a complete mission profile with the help of LUTs. Thus, to overcome the long simulation time issue, the performance of the system is going to be evaluated for one-minute irradiance profiles and would be later used in LUT to evaluate the yearly mission profiles. The mission profile is composed of multiple combinations of irradiance and ambient temperature values throughout the year. The proposed mission profile will consider 10 different irradiance values, from $100W/m^2$ to $1000W/m^2$ in $100W/m^2$ steps which will cover

the irradiance range of the yearly mission profile. It will also consider 10 different temperature values, from $-20°C$ to $25°C$ in $5°C$ steps, which will cover the ambient temperature range of the yearly mission profile. The system will be simulated for each combination of the 10 irradiance and 10 ambient temperature values, with a total of 100 combinations.

From the output values of these simulations, the lifetime consumption and energy production of each combination will be calculated and will be used in the generation of a set of LUTs to evaluate the lifetime consumption and energy generated by the PV system under a year mission profile. The range of irradiance and ambient temperature values for the LUT is selected based on the target mission profile explained in the next subsection.

To evaluate the lifetime consumption and energy generation of the year mission profile, four LUTs were created. Two of the LUTs are for the estimation of the normal MPPT algorithm lifetime consumption and energy generation respectively. The other two LUTs are applied for the estimation of the MTL MPPT algorithm. All of the four LUTs are designed in Matlab Simulink with help of the "Lookup table" block diagram. Each LUT has 2 inputs which are: Irradiance and ambient temperature. The input breakpoints are from a range of $100W/m^2$ to $1000W/m^2$ for the solar irradiance and $-20°C$ to $25°C$ for the ambient temperature. When the irradiance and ambient temperature values match exactly the breakpoints, the output values are directly extracted from the LUTs, when the values do not match exactly the breakpoints values but are within range, the values are calculated through interpolation and when the values are out of the breakpoints range, the output values are estimated by extrapolation. The extrapolation of values has limitation in application, as it loses precision when estimating values that are too far out of range. This is the reason why the LUT breakpoints range were created based of the mission profile application, so most of the mission profile values are within range and the extrapolation is applied just for outliers.

For this work, the target mission profile is a data set from the year 2014 (See Fig. 5.15). The data set is composed of irradiance and ambient temperature values and the time between samples is ten minutes. The mission profile is from Varennes

in Quebec, Canada [50] with a latitude of 45.616084 and longitude -73.386362. Due to the high latitude of the system and the translation movement of the Earth, the irradiance and temperature values during the winter months are low.

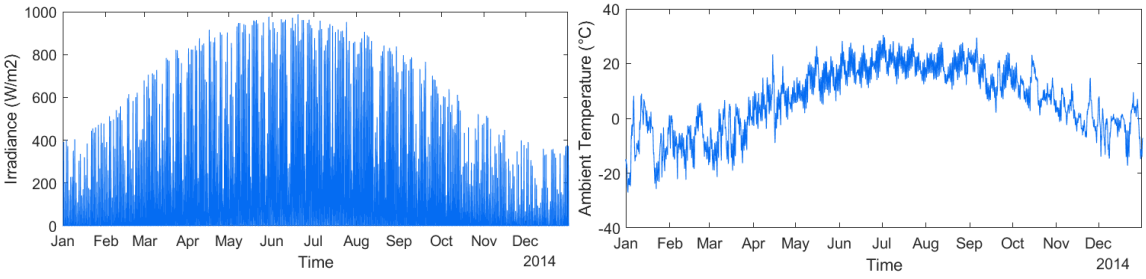

Figure 5.15: Mission profile (Irradiance (a) and Ambient temperature(b)) of the province of Quebec, Canada

Lower power losses come together with lower irradiance levels. Lower irradiance levels along with the lower ambient temperatures cause that the life consumption impact during winter months is negligible compared to summer months. The low temperatures have a positive effect on the solar modules output power which in turn increases the power losses in the switching devices, but the overall junction temperature is reduced as well due to the lower ambient temperatures, having a low damage impact. Contrarily, during the summer months, irradiance levels can reach high values (Up to $1000W/m^2$) causing higher power losses and higher junction temperature in the switching devices. Moreover, higher solar irradiance levels come together with higher ambient temperatures (Up to $25°C$ for this mission profile) and together have a considerable impact on the lifetime consumption of IGBT switching devices.

The results of the application of the MTL MPPT algorithm to the yearly mission profile can be seen in Fig. 5.16. The evaluation of the mission profile was done with the application of the LUTs developed and explained in the previous subsection. The energy production (See Fig. 5.16a) has been reduced principally during summer months when solar irradiance and ambient temperature levels are high. As seen in the previous figures the algorithm have had an effect during the spring season, but the energy production reductions are lower than in summer months due to the lower ambient temperatures. For the life consumption impact, the MTL MPPT algorithm manages to greatly reduce damage received by the IGBT switching devices during

summer months (See Fig. 5.16b) and for the spring season the life consumption is reduced as well, but for the beginning of the spring season as a result of the lower ambient temperatures, the algorithm did not alter much the PV system performance, allowing to harvest more energy during days with high irradiance levels but low ambient temperature.

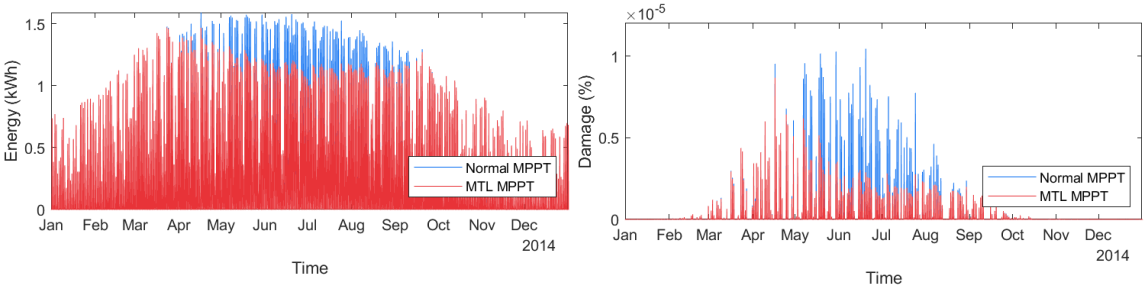

Figure 5.16: Energy generated (a) and lifetime consumption (b) during the year mission profile

The sum of the energy generated during the year mission profile can be seen in Fig. 5.17a, where the energy generated by the PV system with the control a normal and the MTL MPPT algorithms are compared. The MTL MPPT algorithm limited the energy production at specific moments during the working time causing a drop in the energy production. The energy production of the PV system controlled by the MTL MPPT algorithm is 3.97% lower than the PV system controlled by a normal MPPT algorithm. Although, with the limitation of energy production, the thermal stress the power converter was subject to, was reduced as well, causing a drop in the damage received by the system. With the application of the MTL MPPT algorithm, the life consumption was reduced by 28.36% compared to the performance of the system controlled by a normal MPPT algorithm.

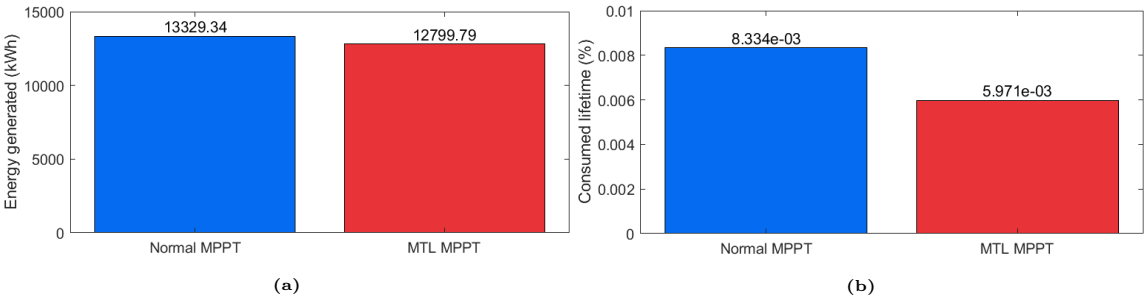

Figure 5.17: Total energy generated (a) and total lifetime consumption (b) during the year mission profile

In this section the MTL MPPT algorithm presented in Chapter 4.2 was applied and tested. To evaluate and compare the performance of the modified MPPT algorithm with a normal MPPT algorithm the lifetime evaluation method explained in Chapter 3 was used. The MTL MPPT algorithm was able to improve the lifetime of a PV system by reducing the maximum temperature that the switching devices could reach. This feature is useful for days with high irradiance and high temperature conditions as the temperature experienced by the device is limited to a certain level and reduces the impact caused by thermal stresses. In the next subsection a Monte Carlo simulation will be applied to have an statistical evaluation that better represents the lifetime of the MTL MPPT algorithm compare with a normal MPPT algorithm.

5.2.1 Monte Carlo simulation

With the application of an empirical lifetime model, it has been possible to estimate the useful lifetime of a PV converter. Despite the precision of the lifetime estimation, in real-life applications the lifetime of IGBT device would vary and be different for each device due to imperfections in materials and construction, as well as different experienced stresses [51]. Therefore, an static lifetime estimation does not represent the end of life of all cases. The random nature of failure and the variations of lifetime due to material and construction imperfections of IGBT devices is better represented with a probabilistic lifetime estimation. Moreover, to evaluate the statistical variations of the lifetime model, a Monte Carlo simulation will be applied in this work.

The Monte Carlo reliability estimation is used to give a probabilistic solution of the problem. The probabilistic solution represents better the random nature of failure in power electronics. The Monte Carlo method relies on the repetition of the solution of the problem many times, where in each repetition some parameters change [24]. The number of repetitions ("n") in this work will be ten thousand times ("$n = 10,000$") for the equation 3.7 . The parameters in the equation (β_1, β_2) will vary the probability density function range established in [13]. The probability density functions of such parameters can be seen in Fig. 5.18.

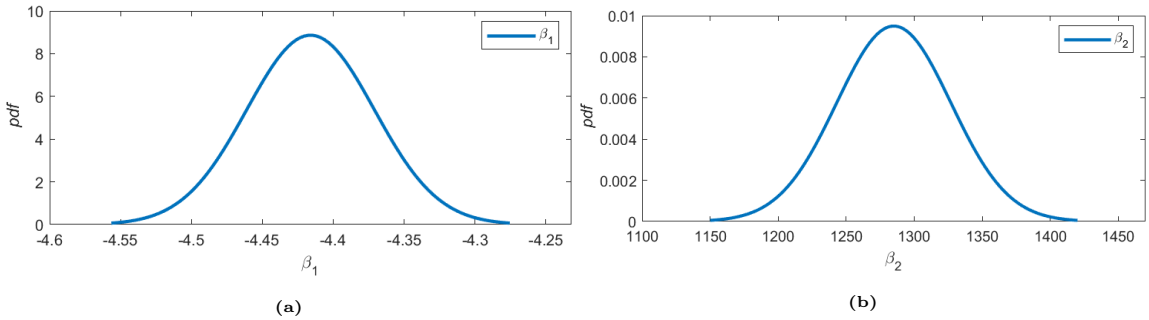

(a) (b)

Figure 5.18: Probability density functions of the parameters under analysis

The lifetime estimation calculated with the empirical lifetime model was obtained based on the thermal stresses experienced by a PV system during a year mission profile. The thermal stress parameters (T_j,ΔT_j,T_{on}) varies continuously through the mission profile, which makes it difficult to apply the Monte Carlo method because the thermal parameters in the solving equation (3.7) are changing constantly. A solution for this problem is to obtain the lifetime consumption for the year mission profile and obtain a set of thermal equivalent static values (T'_j,$\Delta T'_j$,T'_{on}) which would have the same lifetime impact for a year mission profile [22].

To obtain the thermal static values corresponding the lifetime consumption of the year mission profile we will take the lifetime consumption obtained from the empirical lifetime model as a reference to be emulated. The lifetime consumption (LC) of the mission profile evaluated with a normal and the MTL MPPT algorithms are $8.334x10^{-3}$ and $5.971x10^{-3}$ respectively, which are the targets to be matched. The number of cycles to failure is the same for both applications and will be obtained from the multiplication of 365 days, 24 hours, 60 minutes, 60 seconds and 60 Hertz as seen in Table 5.7. The static junction temperature (T'_j) value is obtained from the average junction temperature during the mission profile. Finally, the ($\Delta T'_j$) is calculated with the equation (3.10) and can be seen in Table 5.7.

Once the equivalent static values were obtained it was possible to apply the Monte Carlo simulation. The equation 3.7 was solved 10,000 times with help of the thermal static values and variations of the constant parameters described above. The probabilistic lifetime consumption calculated can be seen in Fig. 5.19 where the solutions of the Monte Carlo simulation were divided into 20 bins. A Weibull probability density function is fitted to the Monte Carlo method output (Red lines

Table 5.7: Parameters for the Monte Carlo Evaluation

Description	Parameter	Value	
		Normal	MTL
Junction temperature	T_j'	53.3968 ($°C$)	52.6978 ($°C$)
Temperature differential	$\Delta T_j'$	4.8349 ($°C$)	4.4919 ($°C$)
Cycle heating time	T_{on}'	0.0083 s	
Number of cycles per year	n	$(365d \cdot 24h \cdot 60m \cdot 60s) \cdot 60Hz$	

in Fig. 5.19).

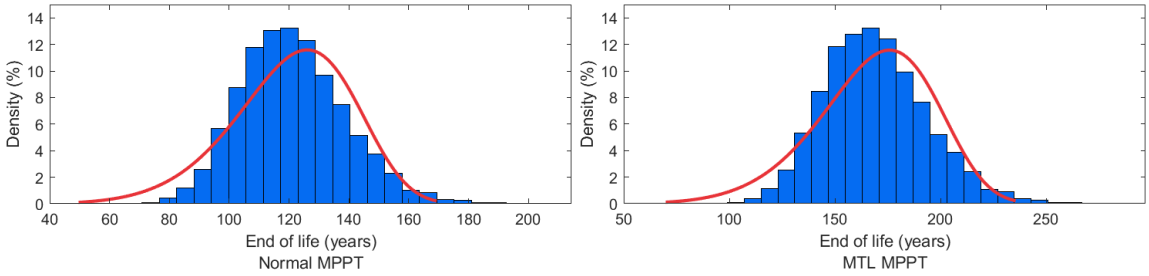

(a) (b)

Figure 5.19: Statistical lifetime estimation with Monte Carlo simulation for normal MPPT (a) and MTL MPPT (b)

After the data is fitted with a Weibull probability density function (PDF) a cumulative density function is implemented to compare the unreliability plots of the normal and MTL MPPT algorithms as seen in Fig. 5.20. When the unreliability plots reach the value of 1 it means that all of the 10,000 samples of the Monte Carlo simulation have reached the end of life. The dashed line in Fig. 5.20 represents the lifetime expected when 10% of the samples have failed. The blue and red lines represent the lifetime of one device of the H-Bridge converter for the normal and MTL MPPT algorithms. For the normal MPPT algorithm a lifetime of 94 years is expected for 10% of cases of one device in the converter, while with the application of the MTL MPPT algorithm, the lifetime is improved to 130 years. It is important to note the lifetime periods are apparently high because just the lifetime of switching devices is being considered (We can see similar results in the evaluation of the effect of the degradation of PV modules [22], where it is suggested that there could be a more precise estimation of the lifetime by including the evaluation of other critical components such as capacitors). For further research the presented approach can

be modified to consider other important elements such as capacitors in the lifetime evaluation. Another implementation can be the comparison of the effect that the presented control method would have for locations with higher irradiance levels.

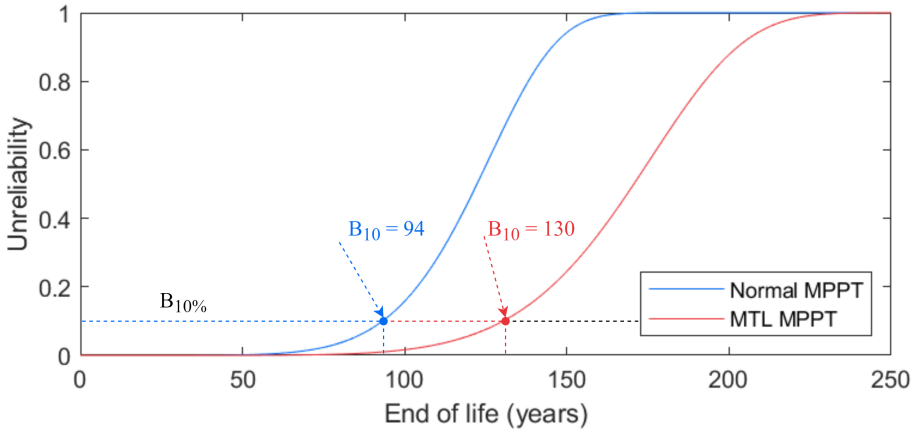

Figure 5.20: Cumulative density function of the Monte Carlo reliability simulation

With the application of the MTL MPPT algorithm, it has been possible to improve the lifetime of a PV converter by reducing the thermal stress that the IGBT switching devices are subject to. The lifetime evaluation carried out in this work have been focused on IGBT switching devices. It is important to mention that other elements of the system can further reduce the lifetime of the PV converter, although they are out of the scope of this study. Finally, this work has demonstrated that the reliability of PV converters can be improved with the application of a thermal management software control method, with no extra implementation costs.

Chapter 6

Conclusions

With the help of digital tools and extensive simulations, this work has demonstrated how the utilization of thermal management control strategies can improve the lifetime period of PV systems with the modification of control software with no extra hardware cost. To evaluate the performance of a PV system and verify the lifetime impact reduction, extensive simulations have been carried out with the help of Matlab and Simulink environments. An empirical lifetime model has been applied to evaluate the lifetime consumption of PV systems. Next, two thermally influenced control algorithms have been proposed and tested. One control algorithm is the temperature-controlled (TC) MPPT algorithm, which regulates the temperature change rate of IGBT devices during dynamic irradiance conditions (cloudy days). The second control algorithm is the maximum-temperature-limited (MTL) MPPT algorithm, which restricts the maximum temperature reached by IGBT devices to reduce the thermal cycling impact and improve lifetime and reliability.

The lifetime modelling technique has been applied and explained step by step. The lifetime modelling included the electrical design of a PV system in Matlab Simulink to emulate its behaviour for various irradiance conditions. It also includes the power loss estimation of the IGBT switching devices; the junction temperature estimation with the use of a thermal model; a rainflow counting algorithm to arrange the random thermal cycles; the empirical lifetime model which use the IGBT thermal cycles to calculate the remaining useful lifetime and it finally includes a Monte Carlo reliability assessment to estimate the reliability of the PV system.

The TC MPPT algorithm (Chapter 4.1) have been applied and tested for daily irradiance profiles for different cloud conditions, it has proved the efficacy of the algorithm to reduce the lifetime impact for very variable cloud conditions, with a life consumption reduction of 4.68% with just 0.08% of energy reduction. For days with variable and overcast cloud conditions, the algorithm did not reduce the life consumption due to the low irradiance changes as previously explained. Finally, for days with clear sky conditions, the algorithm has behaved as expected, with no impact on the performance of the system.

The MTL MPPT algorithm (Chapter 4.2) has been applied and tested for an annual mission profile from the province of Quebec, Canada. The algorithm limits the maximum junction temperature reached by the switching devices. The application of the MTL MPPT algorithm shows that the lifetime consumption of PV system can be reduced 28.36% with a reduction of 3.97% of the energy generated annually. This algorithm limits the temperature of IGBT switching devices by reducing the power generation of the system. The advantage of considering the junction temperature to control the system is that the power is limited based on the power available altogether with the ambient temperature. Considering the ambient temperature helps to limit the power generation when the IGBT has reached a certain limit, and to work at full capacity in case

Moreover, it is important to remark that the lifetime evaluation method applied in this work could be easily modified to be implemented in different locations, different devices or applied the approach with variations on the PV converter topology. Further research can be done for the case of the modified MPPT algorithms. As it is also possible to adapt them to study the impact that the modified algorithms implemented in this work will have in places with harsher environments. Finally, it would be interesting to have more information on the impact that the thermal management control strategies will have on other devices of the PV converter such as capacitors and other semiconductors.

In conclusion, in this work, the use of thermal management control strategies have been applied to improve the lifetime of PV systems. The control strategies proposed were able to reduce the damage received by the PV system considering

the junction temperature of IGBT devices. The TC MPPT algorithm can reduce the temperature change rate during days with very variable cloud conditions and the MTL MPPT algorithm is able to reduce the damage received during days with high irradiance and high ambient temperatures values. As reliability and cost of PV converters are part of the main issues for the development of PV systems, it is important to point that the application of the proposed algorithms could improve the reliability and lifetime of PV systems with the help of software control at no extra hardware cost

Appendix A

Matlab and Simulink

A.1 Function codes

```
#Seach for peaks and valleys to apply the rainflow counting algorithm.
    [pks,locs] = findpeaks(data,x,'MinPeakDistance',0.016); #"x" repesents the
    #location of the datapoints.
    [vks,locidx] = findpeaks(-data,x,'MinPeakDistance',0.016); #"data" is
    #vertically flipped to find valleys.
    vks=-vks;
    #Peaks (pks) and Valleys (vks) are combined.
    pvks((1:length(pks))*2 ) = pks;
    pvks((1:length(vks))*2 - 1) = vks;
    tpvks((1:length(locs))*2 ) = locs;
    tpvks((1:length(locidx))*2 -1) = locidx;
```

```
#Rainflow counting algorithm
    # tpvks and pvks are obtained from the serch of peaks and valleys above
    X = tpvks;
    Y = pvks;
    [c,hist,edges,rmm,idx] = rainflow(Y,X);
```

A.2 Simulink models

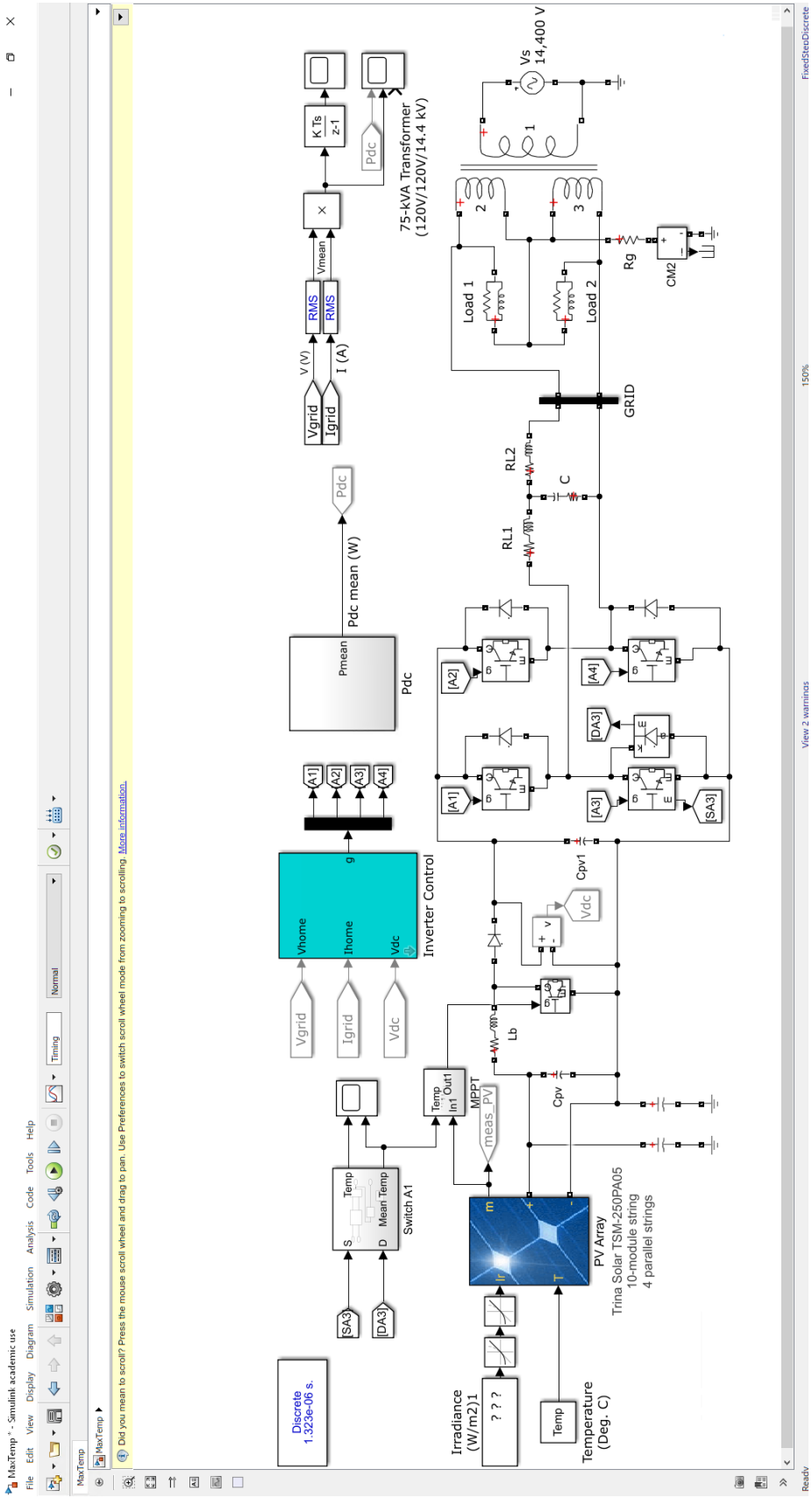

Figure A.1: Diagram of the PV system in Simulink

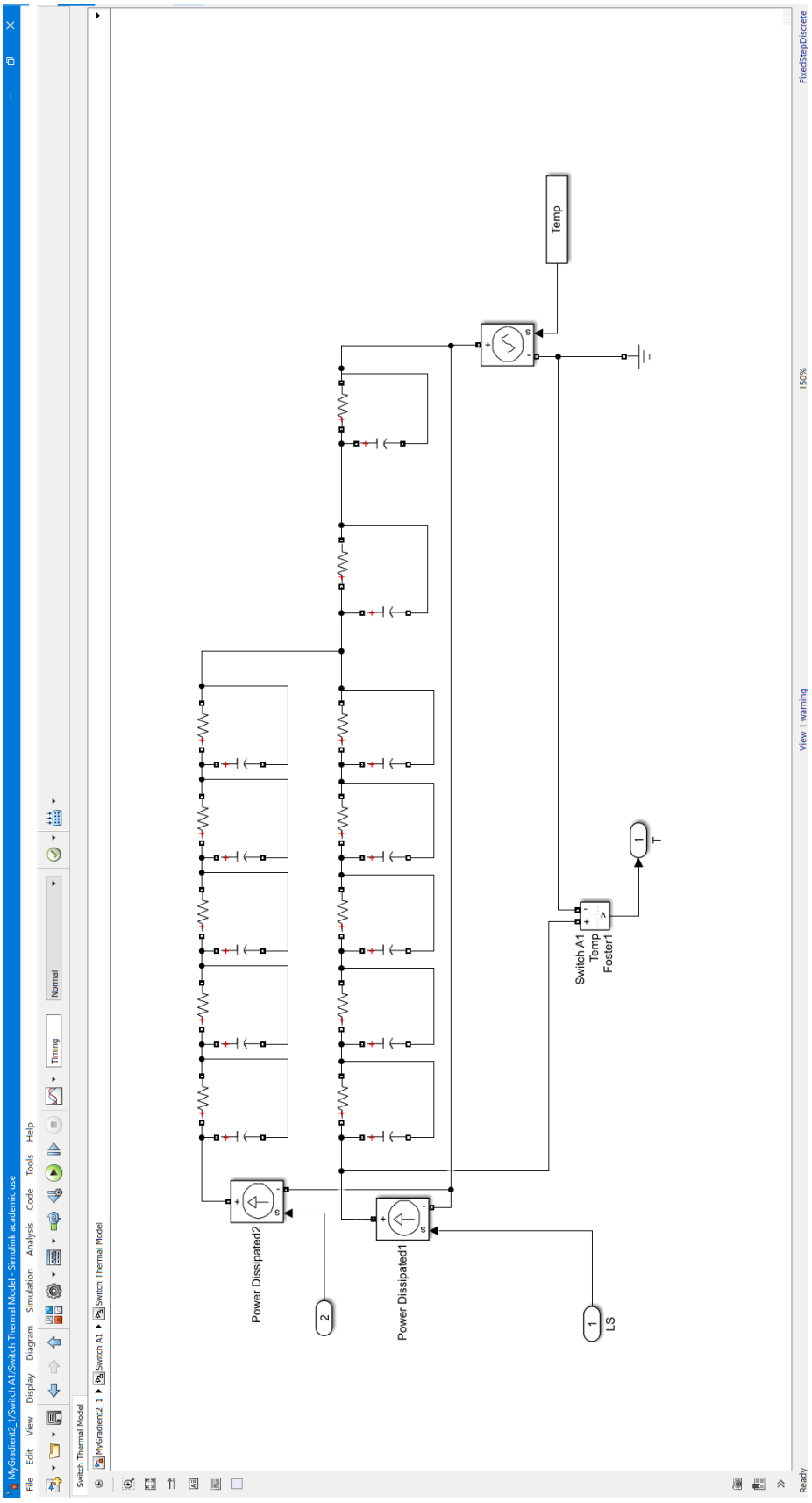

Figure A.2: Diagram of the Foster model in Simulink

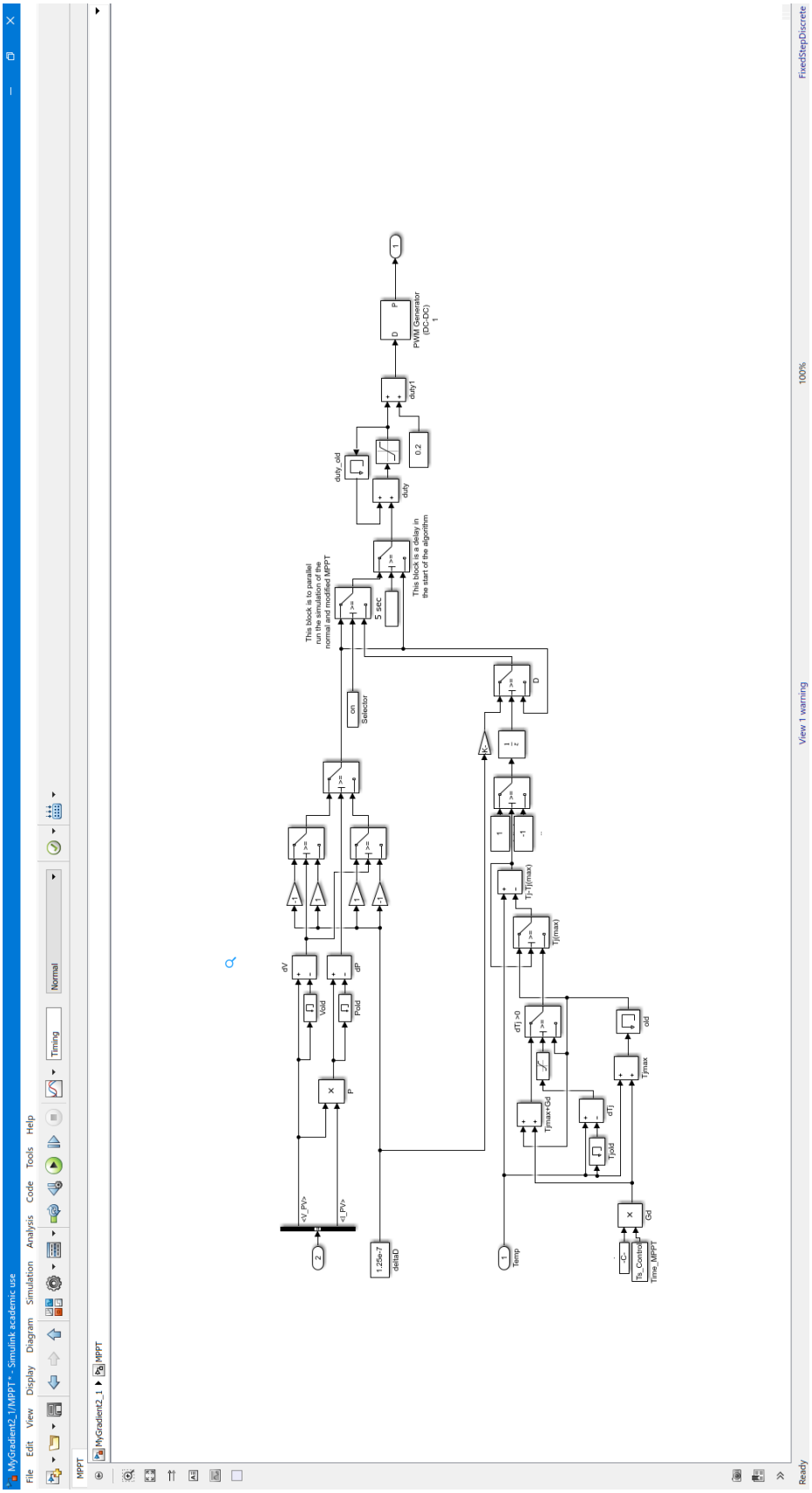

Figure A.3: Diagram of the temperature-controlled MPPT algorithm in Simulink

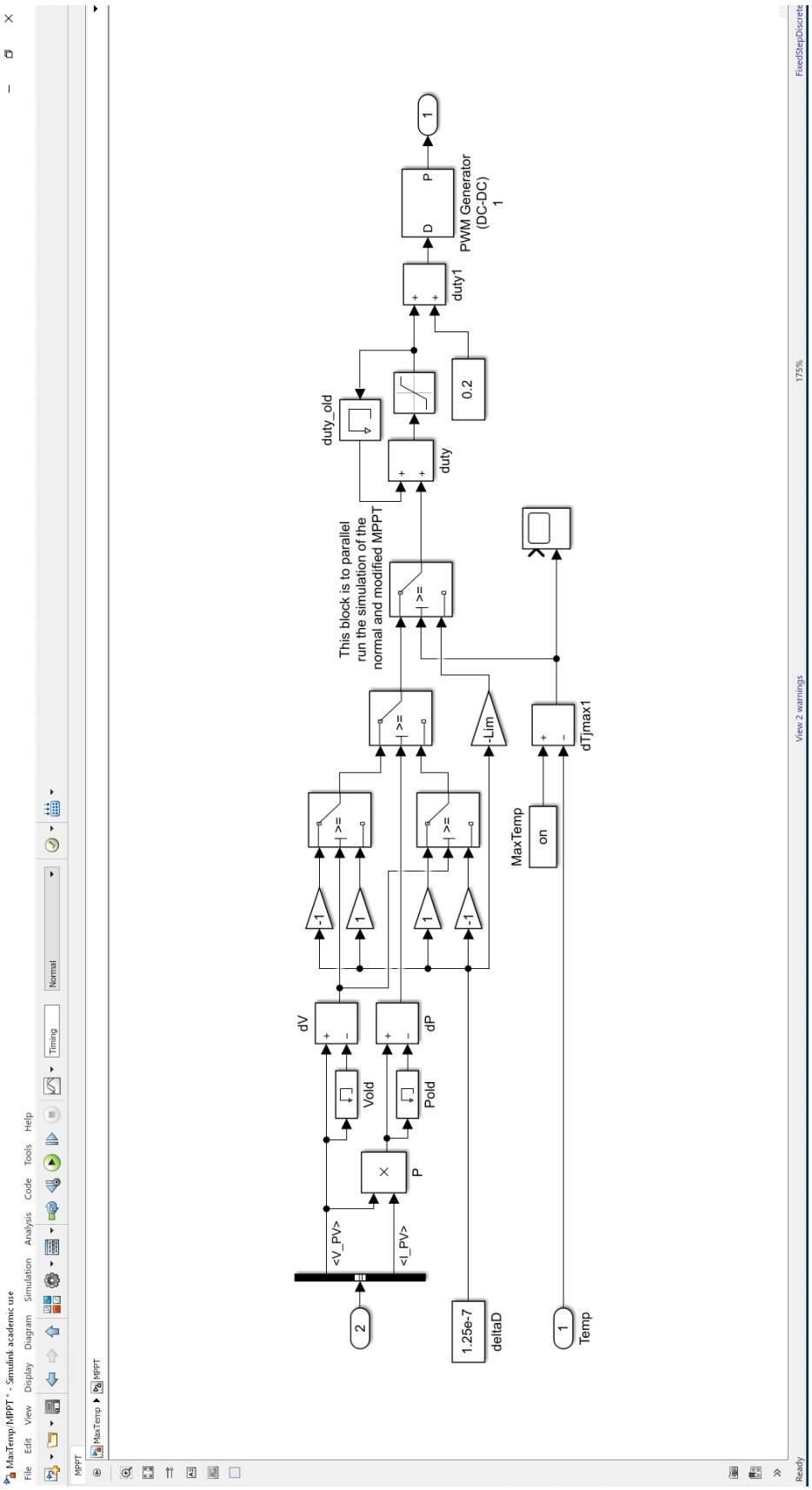

Figure A.4: Diagram of the maximum temperature-limited MPPT algorithm in Simulink

Bibliography

[1] J. Arent, A. Wise, R. Gelman, "The status and prospects of renewable energy for combating global warming," Energy Economics, Volume 33, Issue 4, 2011, Pages 584-593.

[2] M. Malinowski, J. I. Leon and H. Abu-Rub, "Solar Photovoltaic and Thermal Energy Systems: Current Technology and Future Trends," Proceedings of the IEEE, vol. 105, no. 11, pp. 2132-2146, Nov. 2017.

[3] S. Kouro, J. I. Leon, D. Vinnikov and L. G. Franquelo, "Grid-Connected Photovoltaic Systems: An Overview of Recent Research and Emerging PV Converter Technology," IEEE Industrial Electronics Magazine, vol. 9, no. 1, pp. 47-61, March 2015.

[4] H. Wang, M. Liserre and F. Blaabjerg, "Toward Reliable Power Electronics: Challenges, Design Tools, and Opportunities," IEEE Industrial Electronics Magazine, vol. 7, no. 2, pp. 17-26, June 2013.

[5] S. Peyghami, P. Davari and F. Blaabjerg, "System-Level Reliability-Oriented Power Sharing Strategy for DC Power Systems," in IEEE Transactions on Industry Applications, vol. 55, no. 5, pp. 4865-4875, Sept.-Oct. 2019

[6] H. Huang and P. A. Mawby, "A Lifetime Estimation Technique for Voltage Source Inverters," IEEE Transactions on Power Electronics, vol. 28, no. 8, pp. 4113-4119, Aug. 2013.

[7] S. Peyghami, P. Palensky and F. Blaabjerg, "An Overview on the Reliability of Modern Power Electronic Based Power Systems," in IEEE Open Journal of Power Electronics, vol. 1, pp. 34-50, 2020.

[8] J. Falck, C. Felgemacher, A. Rojko, M. Liserre and P. Zacharias, "Reliability of Power Electronic Systems: An Industry Perspective," IEEE Industrial Electronics Magazine, vol. 12, no. 2, pp. 24-35, June 2018.

[9] S. Yang, A. Bryant, P. Mawby, D. Xiang, L. Ran and P. Tavner, "An Industry-Based Survey of Reliability in Power Electronic Converters," in IEEE Transactions on Industry Applications, vol. 47, no. 3, pp. 1441-1451, May-June 2011.

[10] L. Ceccarelli, R. M. Kotecha, A. S. Bahman, F. Iannuzzo and H. A. Mantooth, "Mission-Profile-Based Lifetime Prediction for a SiC mosfet Power Module Using a Multi-Step Condition-Mapping Simulation Strategy," in IEEE Transactions on Power Electronics, vol. 34, no. 10, pp. 9698-9708, Oct. 2019

[11] T. Tomson, "Fast dynamic processes of solar radiation," Solar Energy, vol. 84, no. 2, pp. 318–323, 2010.

[12] M. Held, P. Jacob, G. Nicoletti, P. Scacco and M. -. Poech, "Fast power cycling test of IGBT modules in traction application," Proceedings of Second International Conference on Power Electronics and Drive Systems, 1997, pp. 425-430 vol.1, doi: 10.1109/PEDS.1997.618742.

[13] R. Bayerer, T. Herrmann, T. Licht, j. Lutz and M. Feller, "Model for Power Cycling lifetime of IGBT Modules - various factors influencing lifetime," in 5th International Conference on Integrated Power Electronics Systems, 2008, pp. 1-6.

[14] A. Sangwongwanich, Y. Yang, D. Sera and F. Blaabjerg , "On the Impacts of PV Array Sizing on the Inverter Reliability and Lifetime," IEEE Transactions on Industry Applications, vol. 54, no. 4, pp. 3656-3667, July-Aug. 2018.

[15] H.S. Chung, H. Wang, F. Blaabjerg, and M. Pecht, "Reliability of power electronic converter systems," Energy Engineering, Institution of Engineering and Technology, 2015.

[16] P.D.T. O'connor, "Practical Reliability Engineering," Chichester, United Kingdom, John Wiley ans Sons, Third edition, 1991.

[17] N. Mohan, T.M. Undeland, W.P. Roobins, "Power electronics. Converters, Applications and Design," United States of America, John Wiley and Sons, Third edition, 2003.

[18] H. Wang, K. Ma and F. Blaabjerg, "Design for reliability of power electronic systems," IECON 2012 - 38th Annual Conference on IEEE Industrial Electronics Society, Montreal, QC, pp. 33-44 2012.

[19] M.A. Hannan, M.S. Hossain Lipu, Pin Jern Ker, R.A. Begum, Vasilios G. Agelidis, and F. Blaabjerg". Power electronics contribution to renewable energy conversion addressing emission reduc-tion": Applications, issues, and recommendations.Applied Energy, 251:113404, 2019.

[20] T. Dragičević,, P. Wheeler and F. Blaabjerg, "Artificial Intelligence Aided Automated Design for Reliability of Power Electronic Systems," IEEE Transactions on Power Electronics, vol. 34, no. 8, pp. 7161-7171, Aug. 2019.

[21] A. Anurag, Y. Yang and F. Blaabjerg, "Thermal Performance and Reliability Analysis of Single-Phase PV Inverters With Reactive Power Injection Outside Feed-In Operating Hours," in IEEE Journal of Emerging and Selected Topics in Power Electronics, vol. 3, no. 4, pp. 870-880, Dec. 2015

[22] A. Sangwongwanich, Y. Yang, D. Sera and F. Blaabjerg, "Lifetime Evaluation of Grid-Connected PV Inverters Considering Panel Degradation Rates and Installation Sites," IEEE Transactions on Power Electronics, vol. 33, no. 2, pp. 1225-1236, Feb. 2018.

[23] M. Aly, E. M. Ahmed and M. Shoyama, "Modulation Method for Improving Reliability of Multilevel T-Type Inverter in PV Systems," in IEEE Journal of Emerging and Selected Topics in Power Electronics, vol. 8, no. 2, pp. 1298-1309, June 2020

[24] P. D. Reigosa, H. Wang, Y. Yang and F. Blaabjerb, "Prediction of Bond Wire Fatigue of IGBTs in a PV Inverter Under a Long-Term Operation," IEEE Transactions on Power Electronics, vol. 31, no. 10, pp. 7171-7182, Oct. 2016.

[25] M. Andresen, K. Ma, G. Buticchi, J. Falck, F. Blaabjerg and M. Liserre, "Junction Temperature Control for More Reliable Power Electronics," in IEEE Transactions on Power Electronics, vol. 33, no. 1, pp. 765-776, Jan. 2018

[26] S. Bouguerra, M. R. Yaiche, O. Gassab, A. Sangwongwanich and F. Blaabjerg, "The Impact of PV Panel Positioning and Degradation on the PV Inverter Lifetime and Reliability," in IEEE Journal of Emerging and Selected Topics in Power Electronics.

[27] A. Sangwongwanich, Y. Yang, D. Sera and F. Blaabjerg, "Mission Profile-Oriented Control for Reliability and Lifetime of Photovoltaic Inverters," in IEEE Transactions on Industry Applications, vol. 56, no. 1, pp. 601-610, Jan.-Feb. 2020

[28] S. Peyghami, H. Wang, P. Davari and F. Blaabjerg, "Mission-Profile-Based System-Level Reliability Analysis in DC Microgrids," IEEE Transactions on Industry Applications, vol. 55, no. 5, pp. 5055-5067, Sept.-Oct. 2019.

[29] M. Andresen, G. Buticchi and M. Liserre, "Thermal Stress Analysis and MPPT Optimization of Photovoltaic Systems," IEEE Transactions on Industrial Electronics, vol. 63, no. 8, pp. 4889-4898, Aug. 2016.

[30] M. A. G. de Brito, L. Galotto, L. P. Sampaio, G. d. A. e Melo and C. A. Canesin, "Evaluation of the Main MPPT Techniques for Photovoltaic Applications," in IEEE Transactions on Industrial Electronics, vol. 60, no. 3, pp. 1156-1167, March 2013.

[31] P. Gaur, Y. P. Verma and P. Singh, "Maximum power point tracking algorithms for photovoltaic applications: A comparative study," 2015 2nd International Conference on Recent Advances in Engineering & Computational Sciences (RAECS), 2015, pp. 1-5.

[32] C. Qian et al., "Thermal Management on IGBT Power Electronic Devices and Modules," in IEEE Access, vol. 6, pp. 12868-12884, 2018, doi: 10.1109/ACCESS.2018.2793300.

[33] S. E. De León-Aldaco, H. Calleja, F. Chan and H. R. Jiménez-Grajales, "Effect of the Mission Profile on the Reliability of a Power Converter Aimed at Photovoltaic Applications—A Case Study," in IEEE Transactions on Power Electronics, vol. 28, no. 6, pp. 2998-3007, June 2013

[34] Military Handbook: Reliability Prediction of Electronic Equipment, Standard MIL-HDBK-217F, Dec. 1991.

[35] V. Raveendran, M. Andresen and M. Liserre, "Improving Onboard Converter Reliability for More Electric Aircraft With Lifetime-Based Control," IEEE Transactions on Industrial Electronics, vol. 66, no. 7, pp. 5787-5796, July 2019.

[36] J. He, A. Sangwongwanich, Y. Yang and F. Iannuzzo, "Lifetime Evaluation of Three-Level Inverters for 1500-V Photovoltaic Systems," in IEEE Journal of Emerging and Selected Topics in Power Electronics, doi: 10.1109/JESTPE.2020.3008246.

[37] S. Peyghami, F. Blaabjerg and P. Palensky, "Incorporating Power Electronic Converters Reliability Into Modern Power System Reliability Analysis," in IEEE Journal of Emerging and Selected Topics in Power Electronics, vol. 9, no. 2, pp. 1668-1681, April 2021

[38] M. Musallam, C. M. Johnson, "An Efficient Implementation of the Rainflow Counting algorithm for Life Consumption Estimation," IEEE Transaction on Reliability, vol. 61, no. 4, pp. 978-986, Dec. 2012.

[39] DYNEX, "AN6156 Calculating Power Losses in an IGBT Module," Lincolnshire, United Kingdom, Feb, 2021 [Online]. Available: https://www.dynexsemi.com/Portals/0/assets/downloads/DNX_AN6156.pdf

[40] Infineon Technologies AG, "What SiC package should I choose – a discrete or module package?", Munich, Germany, April, 2021, [Online]. Available: https://www.infineon.com/cms/en/blog/What-SiC-package-should-I-choose-a-discrete-or-module-package/

[41] Infineon Technologies AG, "FS3L50R07W2H3F_B11", Munich, Germany, 2017, [Online]. Available: https://www.infineon.com/dgdl/Infineon-FS3L50R07W2H3F_B11-DataSheet-v03_03-EN.pdf?fileId=db3a30433fe811c7013fec12b85d3c49

[42] Infineon Technologies AG, "Transient Thermal Measurements and thermal equivalent circuit models", Munich, Germany, 2015, [Online]. Available: https://www.infineon.com/dgdl/Infineon-Thermal_equivalent_circuit_models-ApplicationNotes-v01_02-EN.pdf?fileId=db3a30431a5c32f2011aa65358394dd2

[43] R. K. Gatla, W. Chen, G. Zhu, J. V. Wang and S. S. Kshatri, "Lifetime comparison of IGBT modules in Grid-connected Multilevel PV inverters Considering Mission Profile," 2019 10th International Conference on Power Electronics and ECCE Asia (ICPE 2019 - ECCE Asia), Busan, Korea (South), pp. 2764-2769, 2019.

[44] V. V. S. Pradeep Kumar and B. G. Fernandes, "A Fault-Tolerant Single-Phase Grid-Connected Inverter Topology With Enhanced Reliability for Solar PV Applications," in IEEE Journal of Emerging and Selected Topics in Power Electronics, vol. 5, no. 3, pp. 1254-1262, Sept. 2017

[45] M. A. Miner, "Cumulative damage in fatigue," Journal of applied Mechanics. Trans.ASME, vol. 12, pp. A159-A164, 1945.

[46] "Basic Calculation of a Boost Converter's Power Stage," Texas Instruments, Jan, 2014. Accessed on: Feb. 11, 2021.[Online]. Available: Available: https://www.ti.com/lit/an/slva372c/slva372c.pdf?ts=1613010991603

[47] "TSM-PC05 Datasheet," Trina Solar, Nov. 2012. [Online]. Available: https://static.trinasolar.com/sites/default/files/PC05_Datasheet_40mm_EN.pdf

[48] Infineon Technologies AG, "IKW50N60H3", Munich, Germany, 2014, [Online]. Available: https://www.infineon.com/dgdl/Infineon-IKW50N60H3-DataSheet-v02_02-EN.pdf?fileId=db3a30432a40a650012a47934b1e2bea

[49] "High-Resolution Solar Radiation Datasets," Government of Canada, Feb. 18, 2020. Accessed on: Jun. 14, 2020.[Online]. Available: https://www.nrcan.gc.ca/energy/renewable-electricity/solar-photovoltaic/18409

[50] "The Solcast API Toolkit," Solcast. Accessed on: Feb. 2, 2021.[Online]. Available: https://toolkit.solcast.com.au/live-forecast

[51] I. F. Kovacevic-Badstuebner, J. W. Kolar and U. Schilling, "Modelling for the lifetime prediction of power semiconductor modules," in Reliability of Power Electronic Converter Systems, London, United Kingdom, The institution of Engineering and Technology, 2015, pp. 103-140.